Arteriosclerosis, Thrombosis, and Vascular Biology

JOURNAL OF THE AMERICAN HEART ASSOCIATION

Endothelial AMP-Activated Protein Kinase Regulates Blood Pressure and Coronary Flow Responses Through Hyperpolarization Mechanism in Mice

Budbazar Enkhjargal, Shigeo Godo, Ayuko Sawada, Nergui Suvd, Hiroki Saito, Kazuki Noda, Kimio Satoh and Hiroaki Shimokawa

Arterioscler Thromb Vasc Biol. 2014;34:1505-1513; originally published online May 22, 2014;
doi: 10.1161/ATVBAHA.114.303735
Arteriosclerosis, Thrombosis, and Vascular Biology is published by the American Heart Association, 7272 Greenville Avenue, Dallas, TX 75231

Print ISSN: 1079-5642. Online ISSN: 1524-4636

Endothelial AMP-Activated Protein Kinase Regulates Blood Pressure and Coronary Flow Responses Through Hyperpolarization Mechanism in Mice

Budbazar Enkhjargal, Shigeo Godo, Ayuko Sawada, Nergui Suvd, Hiroki Saito, Kazuki Noda, Kimio Satoh, Hiroaki Shimokawa

Objective—Vascular endothelium plays an important role to maintain cardiovascular homeostasis through several mechanisms, including endothelium-dependent hyperpolarization (EDH). We have recently demonstrated that EDH is involved in endothelial metabolic regulation in mice. However, it remains to be examined whether AMP-activated protein kinase (AMPK), an important metabolic regulator, is involved in EDH and if so, whether endothelial AMPK (eAMPK) plays a role for circulatory regulation.

Approach and Results—We examined the role of eAMPK in EDH, using mice with endothelium-specific deficiency of α-catalytic subunit of AMPK, either α_1 (eAMPK$\alpha_1^{-/-}\alpha_2^{+/+}$) or α_2 (eAMPK$\alpha_1^{+/+}\alpha_2^{-/-}$) alone or both of them (eAMPK$\alpha_1^{-/-}\alpha_2^{-/-}$). We performed telemetry, organ chamber, electrophysiological, and Langendorff experiments to examine blood pressure, vascular responses, hyperpolarization of membrane potential, and coronary flow responses, respectively. Hypertension was noted throughout the day in eAMPK$\alpha_1^{-/-}\alpha_2^{-/-}$ and eAMPK$\alpha_1^{-/-}\alpha_2^{+/+}$ but not in eAMPK$\alpha_1^{+/+}\alpha_2^{-/-}$ mice when compared with respective control. Importantly, endothelium-dependent relaxations, EDH, and coronary flow increase were all significantly reduced in eAMPK$\alpha_1^{-/-}\alpha_2^{-/-}$ and eAMPK$\alpha_1^{-/-}\alpha_2^{+/+}$ but not in eAMPK$\alpha_1^{+/+}\alpha_2^{-/-}$ mice. In contrast, endothelium-independent relaxations to sodium nitroprusside (a NO donor), NS-1619 (a Ca^{2+}-activated K^+ channel opener), and exogenous H_2O_2 were almost comparable among the groups. In eAMPK$\alpha_1^{-/-}\alpha_2^{-/-}$ mice, antihypertensive treatment with hydralazine or long-term treatment with metformin (a stimulator of AMPK) failed to restore EDH-mediated responses.

Conclusions—These results provide the first direct evidence that α_1 subunit of eAMPK substantially mediates EDH responses of microvessels and regulates blood pressure and coronary flow responses in mice in vivo, demonstrating the novel role of eAMPK in cardiovascular homeostasis. **(*Arterioscler Thromb Vasc Biol*. 2014;34:1505-1513.)**

Key Words: AMP-activated protein kinases ■ blood pressure ■ endothelial cells ■ endothelium-dependent hyperpolarization factor

Vascular endothelium regulates vascular tone by releasing endothelium-derived relaxing and contracting factors, including nitric oxide (NO), prostacyclin, endothelium-derived hyperpolarizing factor (EDHF), endothelin, and prostaglandin $F_{2\alpha}$, all of which regulate vascular homeostasis through multiple mechanisms. When compared with NO[1] and prostacyclin,[2] relatively little is known about the biochemical, physiological, and pharmacological aspects of endothelium-dependent hyperpolarization (EDH). However, EDHF is considered as one of the important endothelium-derived relaxing factors, especially in resistance arteries.[3,4] During the past 25 years, experiments were performed to clarify the nature of EDHF, identifying several candidates, including K ion, arachidonic acid metabolites, electric gap communications, C-type natriuretic peptide, endogenous cannabinoid, ecto-5′-nucleotidase, and hydrogen sulfide.[5] It is now widely accepted that multiple EDHFs may exist depending on blood vessels and species studied.[6–8] We and others have previously identified that endothelium-derived H_2O_2 is one of the major EDHFs in mouse mesenteric arteries,[9,10] porcine coronary arteries,[11] and human coronary and mesenteric arteries.[12–15] Impaired EDH-type responses have been reported under various pathological conditions, including hypertension, atherosclerosis, hypercholesterolemia, heart failure, ischemia/reperfusion, and diabetes mellitus,[5,16] indicating the important roles of EDH in the maintenance of cardiovascular homeostasis. Furthermore, we have recently demonstrated that endothelium-derived H_2O_2 also plays an important role in endothelial metabolic regulation in mice.[17]

Vascular endothelial dysfunction plays a critical role in the pathogenesis of metabolic syndrome, such as obesity, diabetes mellitus, and hypertension, all of which cause cardiovascular

Received on: March 26, 2014; final version accepted on: May 7, 2014.

From the Department of Cardiovascular Medicine, Tohoku University, Sendai, Japan.

The online-only Data Supplement is available with this article at http://atvb.ahajournals.org/lookup/suppl/doi:10.1161/ATVBAHA.114.303735/-/DC1.

This manuscript was sent to Qingbo Xu, Consulting Editor, for review by expert referees, editorial decision, and final disposition.

Correspondence to Hiroaki Shimokawa, MD, PhD, Department of Cardiovascular Medicine, Tohoku University Graduate School of Medicine, 1-1 Seiryo-Machi, Aoba-ku, Sendai 980-8574, Japan. E-mail shimo@cardio.med.tohoku.ac.jp

Nonstandard Abbreviations and Acronyms

AMPK	AMP-activated protein kinase
eAMPK	endothelial AMP-activated protein kinase
eAMPK-KO	endothelial AMPK knockout
EDH	endothelium-dependent hyperpolarization
EDHF	endothelium-derived hyperpolarizing factor
eNOS	endothelial nitric oxide synthase
L-NNA	N^{ω}-nitro-L-arginine

complications, including myocardial infarction, stroke, and heart and renal failure.[18] Recently, the role of AMP-activated protein kinase (AMPK) has attracted much attention as an important regulator of metabolic functions.[19] AMPK is ubiquitously conserved from yeast to humans, and it is multisubstrate serine/threonine protein kinase involved in the regulation of cellular and whole organism energy homeostasis and metabolism.[20,21] AMPK consists of heterotrimeric complex with a catalytic subunit α and 2 regulatory subunits β and γ,[20] each having ≥2 isoforms (α_1, α_2, β_1, β_2, γ_1, γ_2, and γ_3) that are differentially expressed in various tissues and subcellular locations.[22] In the vascular endothelium, both α subunits of AMPK (α_1 and α_2) are expressed although AMPKα_1 is expressed to a greater extent than AMPKα_2.[22] Previous studies have demonstrated that the predominant isoform expressed in vascular endothelial cells is α_1.[23,24] However, because most studies were performed using systemic knockout or transgenic mice to examine the role of AMPK, the specific role of endothelial AMPK (eAMPK) on endothelium-dependent responses remains to be examined.[25]

Endothelium-dependent vasodilatation is a vital mechanism of blood flow regulation in response to increased metabolic demand. As a metabolic sensor, eAMPK plays an important role in metabolic regulation of blood flow,[24,26] which is also regulated by endothelial NO synthase (eNOS)[27,28] through AMPK activation.[29,30] However, the role of eAMPK in EDH remains to be elucidated. Thus, in the present study, we examined whether eAMPK is involved in EDH and if so, whether it plays a role in blood pressure regulation in mice in vivo.

Materials and Methods

Materials and Methods are available in the online-only Supplement.

Results

Characteristics of Endothelial-Specific AMPK-KO Mice

AMPK is ubiquitously detectable in all cells of organism. To examine the role of eAMPK selectively, we newly generated eAMPK$\alpha_1^{-/-}\alpha_2^{+/+}$, eAMPK$\alpha_1^{+/+}\alpha_2^{-/-}$, and eAMPK$\alpha_1^{-/-}\alpha_2^{-/-}$ mice. We also newly generated each littermate, including control$\alpha_1^{f/f}\alpha_2^{+/+}$, control$\alpha_1^{+/+}\alpha_2^{f/f}$, and control$\alpha_1^{f/f}\alpha\alpha_2^{f/f}$ mice, respectively, because genotype is different in each group. All mice were genotyped by polymerase chain reaction on tail clip samples (Figure IA in the online-only Data Supplement). We also confirmed endothelium-selective knockdown of AMPK isoforms in the aorta, mesenteric, and coronary arteries by immunofluorescence staining method as described in our previous study (Figure 1).[17,31] Characteristics of mice, including body, organ, and fat weights and blood and lipid profiles, are shown in Table I in the online-only Data Supplement. Body weight was significantly decreased in eAMPK$\alpha_1^{-/-}\alpha_2^{-/-}$ and eAMPK$\alpha_1^{-/-}\alpha_2^{+/+}$ mice, but not in eAMPK$\alpha_1^{+/+}\alpha_2^{-/-}$ mice, when compared with each littermate mice. Moreover, heart:body weight ratio was significantly increased in eAMPK$\alpha_1^{-/-}\alpha_2^{-/-}$ and eAMPK$\alpha_1^{-/-}\alpha_2^{+/+}$mice, but not in eAMPK$\alpha_1^{+/+}\alpha_2^{-/-}$ mice, when compared with each littermate mice, indicating that α_1 is the dominant catalytic subunit of endothelial AMPK[23,24,32] related to cardiac hypertrophy. Glucose tolerance was comparable between eAMPK$\alpha_1^{-/-}\alpha_2^{-/-}$ and control$\alpha_1^{f/f}\alpha_2^{f/f}$ mice (Figure IB in the online-only Data Supplement). The weights of other organs and visceral fats were comparable between eAMPK-KO and control mice. This was also the case for blood and lipid profiles (Table I in the online-only Data Supplement).

Role of eAMPK in Blood Pressure Regulation

To study the role of eAMPK in blood pressure regulation in vivo, we monitored blood pressure of eAMPK-KO and control mice by telemetry in vivo. When compared with controls, mean, systolic, and diastolic arterial pressures were significantly higher in eAMPK$\alpha_1^{-/-}\alpha_2^{-/-}$ and eAMPK$\alpha_1^{-/-}\alpha_2^{+/+}$ mice throughout the day but remained unaltered in eAMPK$\alpha_1^{+/+}\alpha_2^{-/-}$ mice (Figure 2; Figure II in the online-only Data Supplement), indicating that eAMPKα_1 plays an important role in blood pressure regulation. In eAMPK-KO mice, heart rate was not

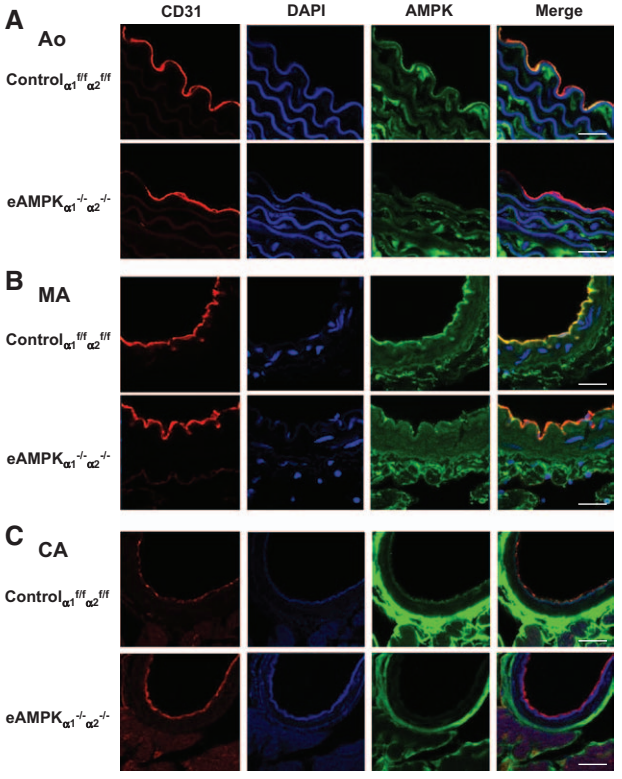

Figure 1. Immunostaining of AMP-activated protein kinase (AMPK) in mouse blood vessels. **A**, Aorta (Ao), (**B**) mesenteric artery (MA), (**C**) coronary artery (CA). Red, CD31; blue, DAPI (4',6-diamidino-2-phenylindole); and green, AMPK. n=3 in each group. Bar, 20 μm.

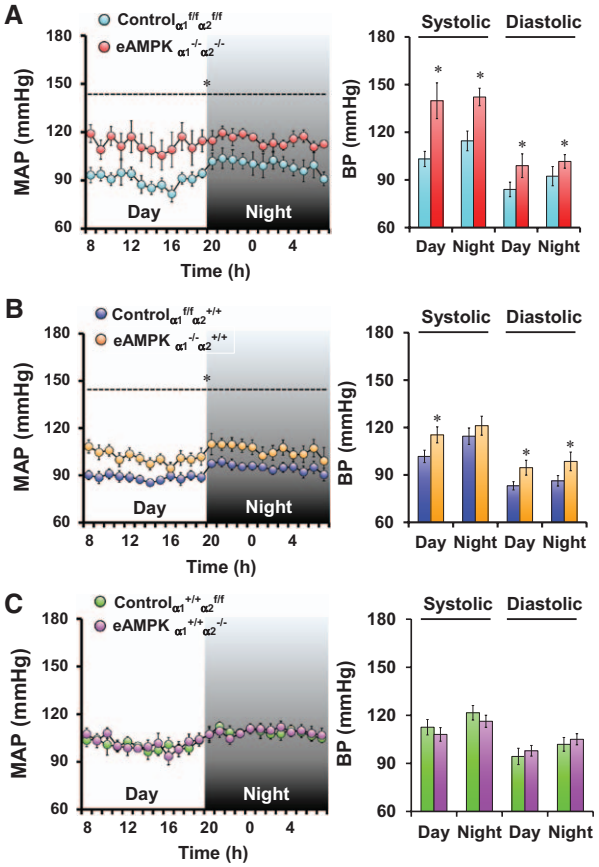

Figure 2. Elevated blood pressure (BP) in eAMPK$\alpha_1^{-/-}\alpha_2^{-/-}$ and eAMPK$\alpha_1^{-/-}\alpha_2^{+/+}$ mice. Telemetric BP monitoring in (**A**) eAMPK$\alpha_1^{-/-}\alpha_2^{-/-}$ vs control$\alpha_1^{f/f}\alpha_2^{f/f}$, (**B**) eAMPK$\alpha_1^{-/-}\alpha_2^{+/+}$ vs control$\alpha_1^{f/f}\alpha_2^{+/+}$, and (**C**) eAMPK$\alpha_1^{+/+}\alpha_2^{-/-}$ vs control$\alpha_1^{+/+}\alpha_2^{f/f}$ (n=5–6 each). Data are presented as mean arterial pressure (MAP) during 24-hour recording (**left**) and time averaged systolic and diastolic BP (**right**). Results are expressed as mean±SEM. *P<0.05 vs control. AMPK indicates AMP-activated protein kinase.

significantly increased in all groups (Figure III in the online-only Data Supplement). Thus, the present results indicate that eAMPKα_1 is the dominant catalytic subunit of AMPK in blood pressure regulation.

eAMPK Regulates EDH Responses

In the organ chamber experiments, we used isolated aorta and mesenteric arteries, which can contract in response to 60 mmol/L of KCl (Figure V in the online-only Data Supplement). In the aorta, acetylcholine-induced endothelium-dependent relaxations were comparable among all eAMPK-KO and control mice, and the responses were inhibited by Nω-nitro-L-arginine (L-NNA; 100 μmol/L, an inhibitor of NOS) and indomethacin (10 μmol/L, an inhibitor of cyclooxygenase; Figure VI in the online-only Data Supplement). However, in mesenteric arteries of control$\alpha_1^{f/f}\alpha_2^{f/f}$ mice, acetylcholine-induced endothelium-dependent relaxations were resistant to L-NNA and indomethacin but were highly sensitive to the combination of apamin and charybdotoxin in the presence of L-NNA and indomethacin, a consistent finding with EDH-mediated relaxations.[9,10,17,33] In contrast, in mesenteric arteries of eAMPK$\alpha_1^{-/-}\alpha_2^{-/-}$ mice, EDH-mediated relaxations to acetylcholine were markedly reduced and the remaining relaxations were inhibited by L-NNA and indomethacin, indicating the compensatory roles of NO and prostacyclin (Figure 3A). Moreover, in mesenteric arteries of eAMPK$\alpha_1^{-/-}\alpha_2^{+/+}$ mice, EDH-mediated relaxations were significantly impaired when compared with control$\alpha_1^{f/f}\alpha_2^{+/+}$ mice (Figure 3B), whereas the same extent of relaxations was noted in both eAMPK$\alpha_1^{+/+}\alpha_2^{-/-}$ and control $\alpha_1^{+/+}\alpha_2^{f/f}$ mice (Figure 3C). In eAMPK$\alpha_1^{-/-}\alpha_2^{-/-}$ mice, endothelium-independent relaxations to sodium nitroprusside (a NO donor) were rather significantly impaired but showed biphasic responses in mesenteric artery (Figure IX in the online-only Data Supplement), whereas NS-1619 (an opener of Ca^{2+}-activated K^+ channel) caused comparable extent of relaxations of the aorta and mesenteric arteries among all the groups (Figure X in the online-only Data Supplement). Furthermore, endothelium-independent relaxations to exogenous H_2O_2 were comparable among the groups (Figure XI in the online-only Data Supplement). Electrophysiological recordings of membrane potentials with the microelectrode technique in the vascular smooth muscle cell of mesenteric arteries demonstrated that EDH to acetylcholine were significantly reduced in eAMPK$\alpha_1^{-/-}\alpha_2^{-/-}$ and eAMPK$\alpha_1^{-/-}\alpha_2^{+/+}$mice when compared with that in respective control mice in the presence of L-NNA and indomethacin (Figure 3D and 3E).

Important Role of eAMPK in Coronary Flow Regulation

Cardiac hypertrophy was noted in eAMPK$\alpha_1^{-/-}\alpha_2^{-/-}$ and eAMPK$\alpha_1^{-/-}\alpha_2^{+/+}$ mice but not in eAMPK$\alpha_1^{+/+}\alpha_2^{-/-}$ mice (Figure 4A; Table I in the online-only Data Supplement). In the Langendorff experiments, baseline coronary flow was significantly increased in eAMPK$\alpha_1^{-/-}\alpha_2^{-/-}$ and eAMPK$\alpha_1^{-/-}\alpha_2^{+/+}$ mice when compared with each control littermates, suggesting the effects of cardiac hypertrophy in these mice (Figure 4B). Importantly, bradykinin-induced endothelium-dependent increases in coronary flow were significantly reduced in eAMPK$\alpha_1^{-/-}\alpha_2^{-/-}$ and eAMPK$\alpha_1^{-/-}\alpha_2^{+/+}$ mice, but not in eAMPK$\alpha_1^{+/+}\alpha_2^{-/-}$ mice, when compared with each control littermates (Figure 4C–4E). In contrast, sodium nitroprusside-induced endothelium-independent responses were comparable between eAMPK-KO mice and controls (Figure 4).

Hydralazine Failed to Restore EDH in eAMPK$\alpha_1^{-/-}\alpha_2^{-/-}$ Mice

eAMPK$\alpha_1^{-/-}\alpha_2^{-/-}$ mice showed high blood pressure throughout the day. After 1-month treatment with hydralazine, blood pressure was significantly decreased in day time but not at night time (Figure IVA and IVB in the online-only Data Supplement), whereas heart rate was unchanged (Figure IVC in the online-only Data Supplement). Cardiac hypertrophy still remained in hydralazine-treated eAMPK$\alpha_1^{-/-}\alpha_2^{-/-}$ mice (Figure IVD; Table II in the online-only Data Supplement). Although endothelium-dependent relaxations were significantly improved in mesenteric arteries (but not in the aorta) in hydralazine-treated eAMPK$\alpha_1^{-/-}\alpha_2^{-/-}$ mice (Figure 5A), this was mainly caused by NO and prostacyclin (Figure VII in the online-only Data Supplement). Hydralazine had no effects on endothelium-independent relaxations to NS-1619 or

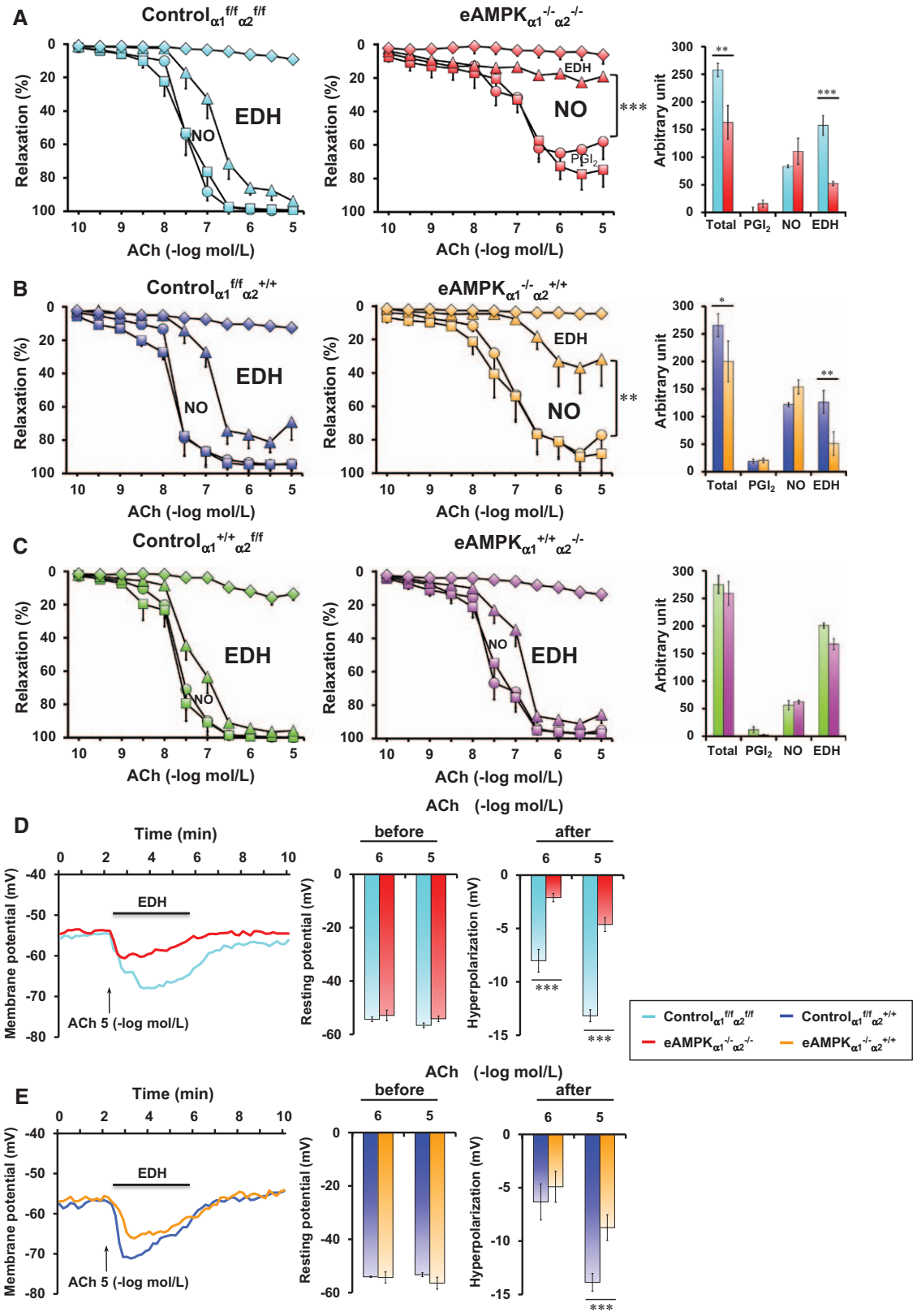

Figure 3. Impaired endothelium-dependent relaxations of mesenteric arteries from endothelial AMP-activated protein kinase knockout (eAMPK-KO) mice. Endothelium-dependent responses to acetylcholine (ACh) in (**A**) eAMPK$\alpha_1^{-/-}\alpha_2^{-/-}$ vs control$\alpha_1^{f/f}\alpha_2^{f/f}$, (**B**) eAMPK$\alpha_1^{-/-}\alpha_2^{+/+}$ vs control$\alpha_1^{f/f}\alpha_2^{+/+}$, and (**C**) eAMPK$\alpha_1^{+/+}\alpha_2^{-/-}$ vs control$\alpha_1^{+/+}\alpha_2^{f/f}$ mice (n=7–10 each) in the absence (○) and the presence of indomethacin (□, Indo), Indo plus N$^{\omega}$-nitro-L-arginine (Δ, L-NNA), and Indo, L-NNA plus charybdotoxin and apamin (lozenge). Data are presented as dose-dependent responses (**left**) and area under the curve (**right**). Representative traces (**left**) of resting membrane potentials and ACh-induced hyperpolarizations in (**D**) eAMPK$\alpha_1^{-/-}\alpha_2^{-/-}$ vs control$\alpha_1^{f/f}\alpha_2^{f/f}$ and (**E**) eAMPK$\alpha_1^{-/-}\alpha_2^{+/+}$ vs control$\alpha_1^{f/f}\alpha_2^{+/+}$ and quantitative results of EDH (**right**; n=7–10 in each). Results are expressed as mean±SEM. $^{**}P<0.01$; $^{***}P<0.001$ vs control. EDH indicates endothelium-dependent hyperpolarization; NO, nitric oxide; and PGI$_2$, prostacyclin.

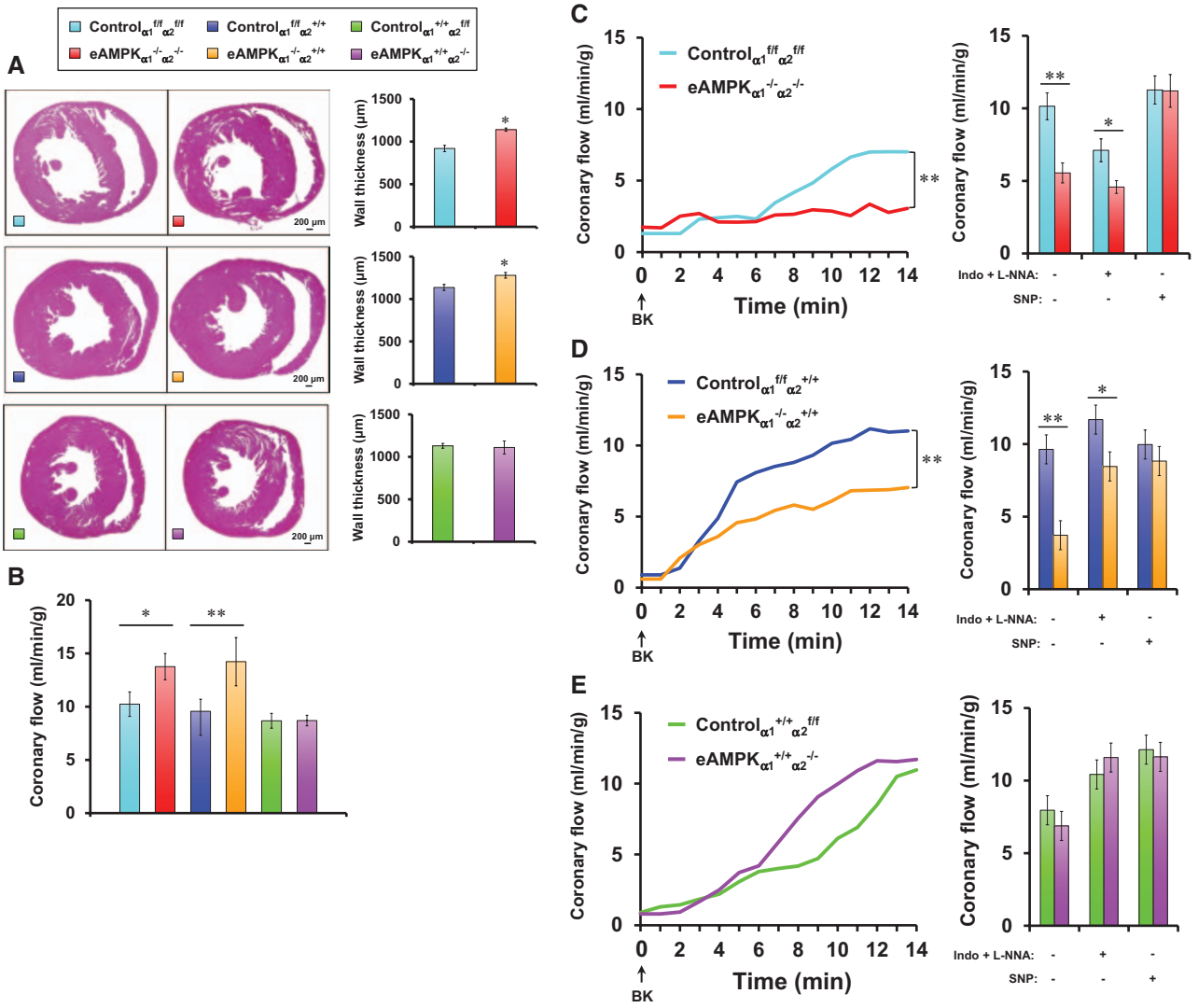

Figure 4. Impaired coronary flow responses in AMP-activated protein kinase knockout (AMPK-KO) mice. **A**, Histological analysis of left ventricular hypertrophy. **B**, Baseline coronary flow of endothelial AMPK (eAMPK)-KO and controls. **C–E**, Coronary flow responses to bradykinin (BK; 1 μmol/L) in Langendorff perfused heart of eAMPK-KO and control mice. Representative traces (**left**, in the presence of indomethacin (Indo) and Nω-nitro-l-arginine [L-NNA]) in (**C**) eAMPK$\alpha_1^{-/-}\alpha_2^{-/-}$ vs control$\alpha_1^{f/f}\alpha_2^{f/f}$, (**D**) eAMPK$\alpha_1^{-/-}\alpha_2^{+/+}$ vs control$\alpha_1^{f/f}\alpha_2^{+/+}$, and (**E**) eAMPK$\alpha_1^{+/+}\alpha_2^{-/-}$ vs control$\alpha_1^{+/+}\alpha_2^{f/f}$ mice and quantitative results of the responses (**right**; n=5 each). Results are expressed as mean±SEM. *P<0.05; **P<0.01 vs control. SNP indicates sodium nitroprusside.

exogenous H_2O_2 in control and eAMPK$\alpha_1^{-/-}\alpha_2^{-/-}$ mice (Figure XII in the online-only Data Supplement).

Metformin Failed to Restore EDH in eAMPK$\alpha_1^{-/-}\alpha_2^{-/-}$ Mice

After 1-month treatment with metformin, blood pressure was significantly decreased during day time but not during night time (Figure IVA and IVB in the online-only Data Supplement), whereas heart rate was unchanged (Figure IVC in the online-only Data Supplement). Cardiac hypertrophy still remained in metformin-treated eAMPK$\alpha_1^{-/-}\alpha_2^{-/-}$ mice (Figure IVD; Table II in the online-only Data Supplement). In eAMPK$\alpha_1^{-/-}\alpha_2^{-/-}$ mice, 1-month treatment with metformin significantly improved endothelium-dependent relaxations of mesenteric arteries but not those of the aorta (Figure 5B). The improvement was mainly mediated by NO and prostacyclin (Figure VIII in the online-only Data Supplement). Metformin had no effects on endothelium-independent relaxations to NS-1619 or exogenous H_2O_2 in control and eAMPK$\alpha_1^{-/-}\alpha_2^{-/-}$ mice (Figure XIII in the online-only Data Supplement). The heart:body weight ratio was unchanged with the metformin treatment (Table II in the online-only Data Supplement).

Discussion

The novel finding of the present study with eAMPK-KO mice was that α_1 subunit of eAMPK plays an important role in EDH responses in resistance arteries and blood pressure control in mice. Although NO and prostacyclin play some compensatory roles, the extent of the compensation was not enough to prevent blood pressure elevation. To the best of our knowledge, this is the first study that demonstrates that eAMPK plays an important role in regulating blood pressure and coronary flow responses through EDH mechanisms (Figure 6).

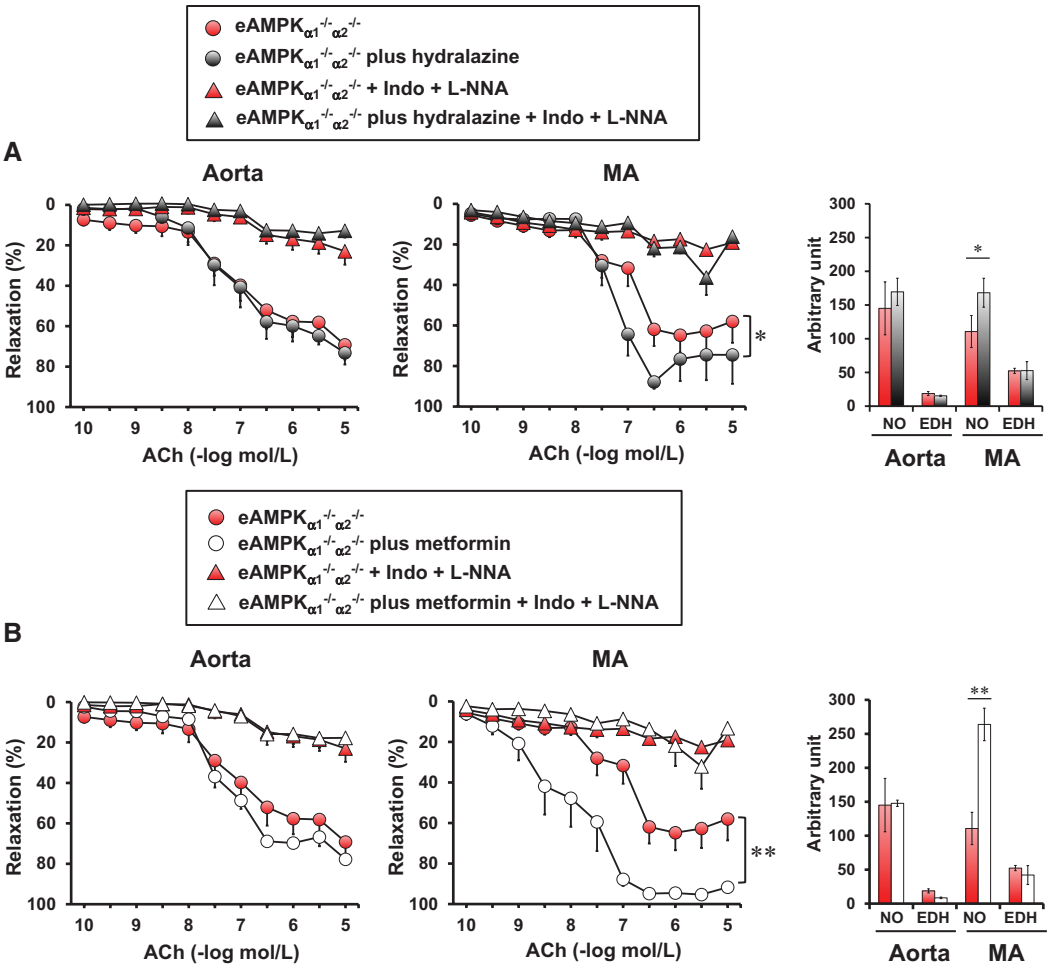

Figure 5. Hydralazine and metformin failed to restore endothelium-dependent hyperpolarization (EDH). Effects of hydralazine (**A**) and metformin (**B**) treatment in the acetylcholine (ACh)–induced EDH-type responses of the aorta and mesenteric arteries (MA), comparing eAMPK$\alpha_1^{-/-}\alpha_2^{-/-}$ plus hydralazine mice and eAMPK$\alpha_1^{-/-}\alpha_2^{-/-}$ plus metformin mice vs eAMPK$\alpha_1^{-/-}\alpha_2^{-/-}$ mice (n=6–7 each) in the absence (○) and the presence of indomethacin (Indo) plus N$^{\omega}$-nitro-L-arginine (L-NNA; Δ). Data are presented as dose-dependent responses (**left**) and area under the curve (**right**). Results are expressed as mean±SEM. *P<0.05; **P<0.01 vs eAMPK$\alpha_1^{-/-}\alpha_2^{-/-}$ mice. Although endothelium-dependent relaxations were significantly improved in MA (but not in the aorta) of eAMPK$\alpha_1^{-/-}\alpha_2^{-/-}$ mice by hydralazine and metformin, this was mainly caused by nitric oxide (NO) and prostacyclin because the improved responses were abolished by Indo and L-NNA. AMPK indicates AMP-activated protein kinase.

Endothelial AMPK Mediates EDH

EDH is mediated by multiple mechanisms involving endothelial and vascular smooth muscle cell components, and several candidates have been proposed as a nature of EDHF, including H_2O_2.[3,6,7,9,34] Recently, Prysyazhna et al[15] showed that dimerization of protein kinase $G_{1\alpha}$ plays an important role in H_2O_2-mediated vascular smooth muscle cell relaxation, which finding was subsequently confirmed in the human coronary artery.[35] We have also previously demonstrated that the 3 NOS isoforms in the endothelium are important sources of H_2O_2 as an EDHF,[3,9,10] and endothelial Cu,Zn-SOD plays an important role as an EDHF synthase,[36] and recently summarized in our findings related to these issues.[37] Interestingly, AMPK is the only kinase that can phosphorylate eNOS on ≥1 site, including Ser1177[30] and Ser633[29] as activating sites in the reductase domain and Thr495 as an inhibitory site in the calmodulin-binding domain.[38,39] Recently, we have demonstrated that eNOS is functionally inhibited under physiological conditions through reduced phosphorylation at Ser1177 and increased phosphorylation at Thr495.[33] In the present study, we were able to demonstrate that endothelial AMPKα_1 substantially mediates EDH in mouse resistance arteries (eg, mesenteric and coronary arteries) but not in the aorta. eNOS is activated in a Ca^{2+}-dependent manner,[40] and NO itself acts as an endogenous activator of AMPK in a Ca^{2+}-dependent manner, involving CaMKKβ.[41] An increase in endothelial Ca^{2+}, crucial step in EDH mechanism,[34,39] activates Ca^{2+}/CaM-dependent protein kinase β with resultant AMPK activation.[42] H_2O_2 could activate endothelial AMPK through Ca^{2+}/CaM-dependent protein kinase β pathway within its physiological concentrations, which could be a possible important feedback mediator of AMPK.[43] In the present study, we found that vascular smooth muscle cell hyperpolarization of mesenteric arteries (in the presence of NO and prostacyclin inhibitors) was significantly impaired in eAMPK-KO mice with reduced relaxation responses, indicating that eAMPK is substantially involved in EDH responses.[44]

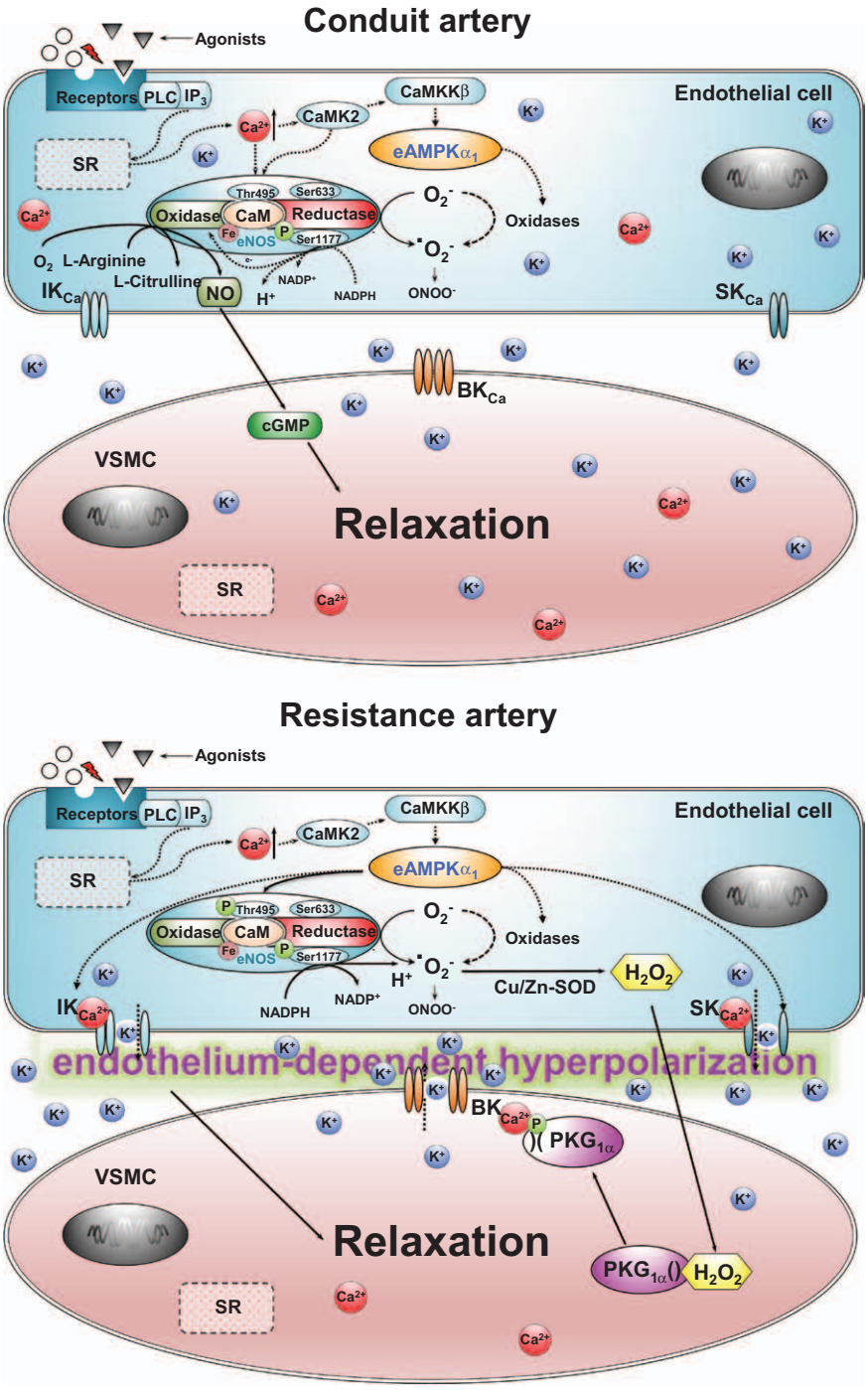

Figure 6. Summary of the present findings. Catalytic subunit α1 of endothelial AMP-activated protein kinase (eAMPK) regulates divergent roles of endothelial nitric oxide synthase (eNOS) in resistance artery. eNOS can also activate eAMPK-independent pathways, including calcium ion (Ca^{2+}), calmodulin (CaM), and Ca^{2+}/CaM-dependent protein kinase 2 (CaMK2)-dependent pathways in conduit artery. BK_{Ca} indicates big conductance K_{Ca}; CaMMKβ, Ca^{2+}/CaM-dependent protein kinase β; e^-, electron; Fe, iron; H^+, hydrogen ion; IK_{Ca}, intermediate K_{Ca}; IP3, inositol triphosphate; K_{Ca}, Ca^{2+} activated potassium (K^+) channel; NADPH, nicotinamide adenine dinucleotide phosphate; O_2^-, superoxide anions; P, phosphorylation; PKG, protein kinase G; PLC, phospholipase C; SK_{Ca} small conductance K_{Ca}; SR, sarcoplasmic reticulum; SOD, superoxide dismutase; and VSMC, vascular smooth muscle cell; arrows, pathways.

Mechanisms of eAMPK-Mediated EDH

Although no drug is currently available to improve EDH-mediated responses directly, beneficial indirect effects of several drugs on EDH-mediated responses have been reported, including angiotensin-converting enzyme inhibitors and angiotensin II type 1 receptor blockers.[5,45] Our previous study showed that EDH component was not restored by the antihypertensive treatment with hydralazine in eNOS-KO mice.[9] In the present study, we found that hydralazine failed to restore EDH-dependent relaxations in mesenteric arteries of eAMPK$\alpha_1^{-/-}\alpha_2^{-/-}$ mice. These results indicate that the impaired EDH-mediated responses in eAMPK$\alpha_1^{-/-}\alpha_2^{-/-}$ mice were not the results of elevated blood pressure but were directly related to eAMPK.

Nonpharmacological therapeutic strategies, including exercise and supplementation with estrogens, ω3-polyunsaturated fatty acids, and polyphenol derivatives have been reported to improve endothelial dysfunction with reduced EDH-mediated responses.[5] Moreover, several pharmacological agents are known to activate AMPK, including glitazones and biguanides, by indirect pathways in whole organism.[24] Metformin, a biguanide derivative, is one of the most commonly used drug for the treatment of type 2 diabetes mellitus.[46] Despite the long historic success

of metformin treatment, its effects on endothelium-dependent responses remain to be examined. It was recently reported that metformin improved vascular dysfunction and increased EDH-mediated relaxations in diabetic rats,[47] and that α_1-subunit of AMPK is involved in the beneficial effects of exercise and prevention of diabetic vascular dysfunction in mice.[48,49] In the present study, metformin failed to restore EDH-mediated responses in mesenteric arteries of eAMPK$\alpha_1^{-/-}\alpha_2^{-/-}$ mice but enhanced the endothelium-dependent compensatory responses mediated by NO and prostacyclin.[47] The present findings could provide clues to develop new therapeutic strategy for the treatment and the prevention of metabolic cardiovascular diseases with a special reference to AMPK.

Limitations

Several limitations should be mentioned for the present study. First, intracellular signaling pathways linking AMPKα_1 and EDH remain to be fully elucidated. In mouse mesenteric and coronary arteries, the major EDHF is H_2O_2 derived from eNOS as we have previously demonstrated.[9,10,17,36] Although we have recently demonstrated the involvement of CaMKKβ, caveolin-1, and AMPK in eNOS activation as an EDHF synthase in mice,[33] the intracellular signaling pathway linking AMPKα_1 and EDH remains to be fully elucidated in future studies. Second, in the present study, we examined the roles of endothelial AMPK in EDH only under normal conditions but not under pathological metabolic conditions, such as diabetes mellitus and hyperlipidemia. Third, glucose tolerance and lipid profiles were fairly preserved in eAMPK$\alpha_1^{-/-}\alpha_2^{-/-}$ mice. It remains to be examined whether some other unknown compensatory mechanisms are involved to maintain glucose tolerance and lipid profiles in those mice.

Clinical Implications

As discussed above, AMPK serves as an important metabolic regulator.[19] Activation of AMPK in whole body is known to exert beneficial effects in obesity, metabolic syndrome, and diabetes mellitus associated with hypertension.[19] However, the long-term effects of systemic activation of AMPK remains controversial, and tissue-specific role of endothelial AMPK remains to be elucidated.[19,22] The present study suggests that genetically induced dysfunction of endothelial AMPK causes EDH impairment with resultant hypertension in mice, suggesting the involvement of dysfunction of endothelial AMPK in the pathogenesis of hypertension and impaired coronary flow responses in patients with metabolic disorder.

In conclusions, we were able to demonstrate that α_1-subunit of eAMPK substantially mediates EDH responses of resistance arteries and thus regulates blood pressure and coronary flow responses in mice in vivo, demonstrating the novel role of eAMPK in cardiovascular homeostasis.

Acknowledgments

We thank Akemi Saito for excellent technical assistance and all members of our laboratory for their contributions to the work. We thank Dr Viollet, Cochin Institute (Paris, France), for providing us with AMP-activated protein kinase floxed mice.

Sources of Funding

This work was supported, in part, by Japanese Scientific Promotion Society grant and a Grant-in-Aid for Scientific Research on Innovative Areas (Signaling Functions of Reactive Oxygen Species), a Grant-in-Aid for Tohoku University Global COE for Conquest of Signal Transduction Diseases with Network Medicine, and Grants-in-Aid for Scientific Research, all of which are from the Ministry of Education, Culture, Sports, Science, and Technology, Tokyo, Japan.

Disclosures

None.

References

1. Furchgott RF, Zawadzki JV. The obligatory role of endothelial cells in the relaxation of arterial smooth muscle by acetylcholine. *Nature*. 1980;288:373–376.
2. Moncada S, Vane JR. The role of prostacyclin in vascular tissue. *Fed Proc*. 1979;38:66–71.
3. Shimokawa H. Hydrogen peroxide as an endothelium-derived hyperpolarizing factor. *Pflugers Arch*. 2010;459:915–922.
4. Shimokawa H, Yasutake H, Fujii K, Owada MK, Nakaike R, Fukumoto Y, Takayanagi T, Nagao T, Egashira K, Fujishima M, Takeshita A. The importance of the hyperpolarizing mechanism increases as the vessel size decreases in endothelium-dependent relaxations in rat mesenteric circulation. *J Cardiovasc Pharmacol*. 1996;28:703–711.
5. Félétou M, Vanhoutte PM. EDHF: an update. *Clin Sci (Lond)*. 2009;117:139–155.
6. Campbell WB, Gauthier KM. Inducible endothelium-derived hyperpolarizing factor: role of the 15-lipoxygenase-EDHF pathway. *J Cardiovasc Pharmacol*. 2013;61:176–187.
7. Dora KA. Coordination of vasomotor responses by the endothelium. *Circ J*. 2010;74:226–232.
8. Félétou M, Vanhoutte PM. Endothelium-dependent hyperpolarization: no longer an f-word! *J Cardiovasc Pharmacol*. 2013;61:91–92.
9. Matoba T, Shimokawa H, Nakashima M, Hirakawa Y, Mukai Y, Hirano K, Kanaide H, Takeshita A. Hydrogen peroxide is an endothelium-derived hyperpolarizing factor in mice. *J Clin Invest*. 2000;106:1521–1530.
10. Takaki A, Morikawa K, Tsutsui M, Murayama Y, Tekes E, Yamagishi H, Ohashi J, Yada T, Yanagihara N, Shimokawa H. Crucial role of nitric oxide synthases system in endothelium-dependent hyperpolarization in mice. *J Exp Med*. 2008;205:2053–2063.
11. Matoba T, Shimokawa H, Morikawa K, Kubota H, Kunihiro I, Urakami-Harasawa L, Mukai Y, Hirakawa Y, Akaike T, Takeshita A. Electron spin resonance detection of hydrogen peroxide as an endothelium-derived hyperpolarizing factor in porcine coronary microvessels. *Arterioscler Thromb Vasc Biol*. 2003;23:1224–1230.
12. Liu Y, Bubolz AH, Mendoza S, Zhang DX, Gutterman DD. H2O2 is the transferrable factor mediating flow-induced dilation in human coronary arterioles. *Circ Res*. 2011;108:566–573.
13. Matoba T, Shimokawa H, Kubota H, Morikawa K, Fujiki T, Kunihiro I, Mukai Y, Hirakawa Y, Takeshita A. Hydrogen peroxide is an endothelium-derived hyperpolarizing factor in human mesenteric arteries. *Biochem Biophys Res Commun*. 2002;290:909–913.
14. Miura H, Bosnjak JJ, Ning G, Saito T, Miura M, Gutterman DD. Role for hydrogen peroxide in flow-induced dilation of human coronary arterioles. *Circ Res*. 2003;92:e31–e40.
15. Prysyazhna O, Rudyk O, Eaton P. Single atom substitution in mouse protein kinase G eliminates oxidant sensing to cause hypertension. *Nat Med*. 2012;18:286–290.
16. Yada T, Shimokawa H, Hiramatsu O, Haruna Y, Morita Y, Kashihara N, Shinozaki Y, Mori H, Goto M, Ogasawara Y, Kajiya F. Cardioprotective role of endogenous hydrogen peroxide during ischemia-reperfusion injury in canine coronary microcirculation in vivo. *Am J Physiol Heart Circ Physiol*. 2006;291:H1138–H1146.
17. Nakajima S, Ohashi J, Sawada A, Noda K, Fukumoto Y, Shimokawa H. Essential role of bone marrow for microvascular endothelial and metabolic functions in mice. *Circ Res*. 2012;111:87–96.
18. Vanhoutte PM, Shimokawa H, Tang EH, Feletou M. Endothelial dysfunction and vascular disease. *Acta Physiol (Oxf)*. 2009;196:193–222.
19. Viollet B, Andreelli F. AMP-activated protein kinase and metabolic control. *Handb Exp Pharmacol*. 2011;203:303–330

20. Kahn BB, Alquier T, Carling D, Hardie DG. AMP-activated protein kinase: ancient energy gauge provides clues to modern understanding of metabolism. *Cell Metab*. 2005;1:15–25.
21. Lamia KA, Sachdeva UM, DiTacchio L, Williams EC, Alvarez JG, Egan DF, Vasquez DS, Juguilon H, Panda S, Shaw RJ, Thompson CB, Evans RM. AMPK regulates the circadian clock by cryptochrome phosphorylation and degradation. *Science*. 2009;326:437–440.
22. Ewart MA, Kennedy S. AMPK and vasculoprotection. *Pharmacol Ther*. 2011;131:242–253.
23. Davis BJ, Xie Z, Viollet B, Zou MH. Activation of the AMP-activated kinase by antidiabetes drug metformin stimulates nitric oxide synthesis *in vivo* by promoting the association of heat shock protein 90 and endothelial nitric oxide synthase. *Diabetes*. 2006;55:496–505.
24. Zou MH, Kirkpatrick SS, Davis BJ, Nelson JS, Wiles WG IV, Schlattner U, Neumann D, Brownlee M, Freeman MB, Goldman MH. Activation of the AMP-activated protein kinase by the anti-diabetic drug metformin in vivo. Role of mitochondrial reactive nitrogen species. *J Biol Chem*. 2004;279:43940–43951.
25. Viollet B, Athea Y, Mounier R, Guigas B, Zarrinpashneh E, Horman S, Lantier L, Hebrard S, Devin-Leclerc J, Beauloye C, Foretz M, Andreelli F, Ventura-Clapier R, Bertrand L. AMPK: Lessons from transgenic and knockout animals. *Front Biosci (Landmark Ed)*. 2009;14:19–44.
26. Goirand F, Solar M, Athea Y, Viollet B, Mateo P, Fortin D, Leclerc J, Hoerter J, Ventura-Clapier R, Garnier A. Activation of AMP kinase alpha1 subunit induces aortic vasorelaxation in mice. *J Physiol*. 2007;581(Pt 3):1163–1171.
27. Dudzinski DM, Michel T. Life history of eNOS: partners and pathways. *Cardiovasc Res*. 2007;75:247–260.
28. Förstermann U, Münzel T. Endothelial nitric oxide synthase in vascular disease: from marvel to menace. *Circulation*. 2006;113:1708–1714.
29. Chen Z, Peng IC, Sun W, Su MI, Hsu PH, Fu Y, Zhu Y, DeFea K, Pan S, Tsai MD, Shyy JY. AMP-activated protein kinase functionally phosphorylates endothelial nitric oxide synthase Ser633. *Circ Res*. 2009;104:496–505.
30. Chen ZP, Mitchelhill KI, Michell BJ, Stapleton D, Rodriguez-Crespo I, Witters LA, Power DA, Ortiz de Montellano PR, Kemp BE. AMP-activated protein kinase phosphorylation of endothelial NO synthase. *FEBS Lett*. 1999;443:285–289.
31. Satoh K, Nigro P, Matoba T, O'Dell MR, Cui Z, Shi X, Mohan A, Yan C, Abe J, Illig KA, Berk BC. Cyclophilin A enhances vascular oxidative stress and the development of angiotensin II-induced aortic aneurysms. *Nat Med*. 2009;15:649–656.
32. Zarrinpashneh E, Carjaval K, Beauloye C, Ginion A, Mateo P, Pouleur AC, Horman S, Vaulont S, Hoerter J, Viollet B, Hue L, Vanoverschelde JL, Bertrand L. Role of the α2-isoform of AMP-activated protein kinase in the metabolic response of the heart to no-flow ischemia. *Am J Physiol*. 2006;291:H2875–2883.
33. Ohashi J, Sawada A, Nakajima S, Noda K, Takaki A, Shimokawa H. Mechanisms for enhanced endothelium-derived hyperpolarizing factor-mediated responses in microvessels in mice. *Circ J*. 2012;76:1768–1779.
34. Enkhjargal B, Hashimoto M, Sakai Y, Shido O. Characterization of vasoconstrictor-induced relaxation in the cerebral basilar artery. *Eur J Pharmacol*. 2010;637:118–123.
35. Zhang DX, Borbouse L, Gebremedhin D, Mendoza SA, Zinkevich NS, Li R, Gutterman DD. H_2O_2-induced dilation in human coronary arterioles: role of protein kinase G dimerization and large-conductance Ca^{2+}-activated K^+ channel activation. *Circ Res*. 2012;110:471–480.
36. Morikawa K, Shimokawa H, Matoba T, Kubota H, Akaike T, Talukder MA, Hatanaka M, Fujiki T, Maeda H, Takahashi S, Takeshita A. Pivotal role of Cu,Zn-superoxide dismutase in endothelium-dependent hyperpolarization. *J Clin Invest*. 2003;112:1871–1879.
37. Satoh K, Godo S, Saito H, Enkhjargal B, Shimokawa H. Dual roles of vascular-derived reactive oxygen species with special reference to hydrogen peroxide and cyclophillin A. *J Mol Cell Cardiol*. 2014. doi: 10.1016/j.yjmcc.2013.12.022.
38. Fisslthaler B, Fleming I. Activation and signaling by the AMP-activated protein kinase in endothelial cells. *Circ Res*. 2009;105:114–127.
39. Michell BJ, Chen Zp, Tiganis T, Stapleton D, Katsis F, Power DA, Sim AT, Kemp BE. Coordinated control of endothelial nitric-oxide synthase phosphorylation by protein kinase C and the cAMP-dependent protein kinase. *J Biol Chem*. 2001;276:17625–17628.
40. Fleming I, Busse R. Signal transduction of eNOS activation. *Cardiovasc Res*. 1999;43:532–541.
41. Zhang J, Xie Z, Dong Y, Wang S, Liu C, Zou MH. Identification of nitric oxide as an endogenous activator of the AMP-activated protein kinase in vascular endothelial cells. *J Biol Chem*. 2008;283:27452–27461.
42. Stahmann N, Woods A, Carling D, Heller R. Thrombin activates AMP-activated protein kinase in endothelial cells via a pathway involving Ca^{2+}/calmodulin-dependent protein kinase kinase beta. *Mol Cell Biol*. 2006;26:5933–5945.
43. Jin BY, Sartoretto JL, Gladyshev VN, Michel T. Endothelial nitric oxide synthase negatively regulates hydrogen peroxide-stimulated AMP-activated protein kinase in endothelial cells. *Proc Natl Acad Sci U S A*. 2009;106:17343–17348.
44. Bryan RM Jr, You J, Golding EM, Marrelli SP. Endothelium-derived hyperpolarizing factor: a cousin to nitric oxide and prostacyclin. *Anesthesiology*. 2005;102:1261–1277.
45. Fujiki T, Shimokawa H, Morikawa K, Kubota H, Hatanaka M, Talukder MA, Matoba T, Takeshita A, Sunagawa K. Endothelium-derived hydrogen peroxide accounts for the enhancing effect of an angiotensin-converting enzyme inhibitor on endothelium-derived hyperpolarizing factor-mediated responses in mice. *Arterioscler Thromb Vasc Biol*. 2005;25:766–771.
46. Knowler WC, Barrett-Connor E, Fowler SE, Hamman RF, Lachin JM, Walker EA, Nathan DM; Diabetes Prevention Program Research Group. Reduction in the incidence of type 2 diabetes with lifestyle intervention or metformin. *N Engl J Med*. 2002;346:393–403.
47. Matsumoto T, Noguchi E, Ishida K, Kobayashi T, Yamada N, Kamata K. Metformin normalizes endothelial function by suppressing vasoconstrictor prostanoids in mesenteric arteries from OLETF rats, a model of type 2 diabetes. *Am J Physiol Heart Circ Physiol*. 2008;295:H1165–H1176.
48. Kröller-Schön S, Jansen T, Hauptmann F, Schüler A, Heeren T, Hausding M, Oelze M, Viollet B, Keaney JF Jr, Wenzel P, Daiber A, Münzel T, Schulz E. α1AMP-activated protein kinase mediates vascular protective effects of exercise. *Arterioscler Thromb Vasc Biol*. 2012;32:1632–1641.
49. Li FY, Lam KS, Tse HF, Chen C, Wang Y, Vanhoutte PM, Xu A. Endothelium-selective activation of AMP-activated protein kinase prevents diabetes mellitus-induced impairment in vascular function and reendothelialization via induction of heme oxygenase-1 in mice. *Circulation*. 2012;126:1267–1277.

Significance

Vascular endothelial dysfunction plays a critical role in the pathogenesis of metabolic syndrome, where AMP-activated protein kinase (AMPK) plays important roles as a metabolic sensor. However, because the systemic AMPK double knockout mice are embryonic lethal, the specific role of endothelial AMPK (eAMPK) remains to be elucidated. To address this important issue, we newly generated endothelium-specific eAMPK-knockout mice and examined the roles of eAMPK in endothelium-dependent responses. In the present study, we were able to demonstrate that eAMPKα_1 is the main upstream enzyme that mediates endothelium-dependent hyperpolarization in resistance arteries, including the coronary and mesenteric arteries for blood pressure regulation and coronary flow responses, respectively, demonstrating the novel role of eAMPK in cardiovascular homeostasis.

Materials and Methods

Animals

This study was reviewed and approved by the Committee on Ethics of Animal Experiments of Tohoku University. We generated eAMPK$_{\alpha1}^{-/-}{}_{\alpha2}^{+/+}$, eAMPK$_{\alpha1}^{+/+}{}_{\alpha2}^{-/-}$ and eAMPK$_{\alpha1}^{-/-}{}_{\alpha2}^{-/-}$ mice by crossing AMPK floxed (f) mice[1] with Tie2-Cre mice[2] on a C57BL/6 background of both mice. Each littermate was used as controls (control$_{\alpha1}^{f/f}{}_{\alpha2}^{+/+}$, control$_{\alpha1}^{+/+}{}_{\alpha2}^{f/f}$ and control$_{\alpha1}^{f/f}{}_{\alpha2}^{f/f}$, respectively). The genotype of the mice was confirmed by polymerase chain reaction using primers specific for the AMPKα_1 gene (5`-TATTGCTGCCATTAGGCTAC-3` and 5`-GACCTGACAGAATAGGATATGCCCAACCTC-3`), the AMPKα_2 gene (5`-GCTTAGCACGTTACCCTGGATGG-3` and 5`-GTTATCAGCCCAACTAATTACAC-3`) and the Tie2-Cre transgene (5`-GCGGTCTGGCAGTAAAAACTATC-3` and 5`-GTGAAACAGCATTGCTGTCACTT-3`). DNAs were amplified 35 cycles at 94ºC for 30 sec, 58ºC for 40 sec and 72ºC for 50 sec in a thermal cycler. Tie2-Cre mice were purchased from Jackson Laboratory. Heterozygous mice backcrossed 4-6 times to fix genotypes and all experiments were performed with generation F4-6. In the present study, we only used male mice. They were maintained on 23±2ºC, 50±10% relative humidity, 12/12 hour light/dark cycle, 13-15 cycles of air exchange and received standard rodent diet (CE-II, Labo MR Stock, Nosan Corporation, Yokohama, Japan) and water *ad libitum*. Male eAMPK-KO mice and each littermate mice, 16-20 weeks old, were used in the present study.

Telemetry experiments in vivo

The mice were anesthetized with 1.5-2 % escain in 190-200 mL of O_2 per minute with postoperative analgesia by carprofen 5 mg/kg, which carprofen was once administered subcutaneously. The sufficiency of anesthesia was determined by the respiration rate and the absence of the blink and paw pinch reflex. At week 3, a telemetry probe catheter (TA11PA-C10, Data Science International, St. Paul, MN, USA) was implanted into the aortic arch through the left carotid artery. All surgeries were performed using sterile technique and after the operation, the animals were treated with cefazolin 100 mg/kg for 3 days. They were housed individually for 1 week on top of the telemetry receivers to allow environmental adaptation before telemetry recording.

Organ chamber experiments

The mice were euthanized by intraperitoneal pentobarbital (50 mg/kg) anesthesia. The aorta and the first branches of mesenteric arteries were isolated and immersed in ice cold Krebs-Henseleit buffer (KHB) bubbled with 95% O_2 and 5% CO_2. The aorta and mesenteric arteries (200-250 μm in diameter) were cut into 0.9-1.0 mm long segments and threaded onto 40 μm steel and 30 μm tungsten wires, respectively. Then, the aorta and mesenteric arteries were loaded with 7-7.5 and 3-3.5 mN resting tension, respectively, which are optimal tension that induces a constant contractile response to 60 mmol/L KCl, as previously demonstrated.[3] Each segment was

mounted in an organ chamber of isometric myograph (620M, Danish Myo Technology, Aarhus, Denmark) and was equilibrated for 1 hour. Experiments were monitored by a computer-based analysis system in Mac-Lab and Chart 7.0 software. After 1 hour equilibration, the preparations were stimulated with 60 mmol/L KCl solution, in which part of NaCl had been replaced by an equimolar amount of KCl, containing (mmol/L) NaCl 22.6, KCl 98.8, $NaHCO_3$ 25, $MgSO_4$ 1.2, KH_2PO_4 1.2, $CaCl_2$, 1.2, glucose 10 at pH 7.4 and 37℃. After washout and 30 min recovery, the preparations were exposed to agonists and cumulative doses were added to organ chambers at 2-3 min intervals.

Electrophysiological experiments

The rings of small mesenteric arteries were placed in experimental chambers perfused with 37 ℃ KHB containing indomethacin (10 μmol/L) and L-NNA (100 μmol/L) bubbled with 95% O_2 and 5% CO_2. A fine glass capillary microelectrode was impaled into the smooth muscle from the adventitial side of mesenteric arteries, and changes in membrane potential were continuously recorded as previously described.[4,5]

Langendorff experiments

After 10 min heparinization (500 units IP), the mice were anesthetized with 50 mg/kg pentobarbital sodium injected intraperitoneally and thoracotomy was performed and the lungs with the trachea were removed, and the hearts were isolated rapidly from the animals. The hearts were then quickly excised and placed in ice-cold KHB including 0.5 mmol/L EDTA to arrest cardiac contraction. After all extracardiac tissues were removed, the aorta was carefully tied to an aortic cannula with a 21-gauge blunted needle within 5 min. The heart was perfused retrogradely by constant 1.8-2 ml/min flow at a constant pressure of 80 mmHg with warm KHB and was allowed to beat once more spontaneously. After the stabilization period, the heart was paced at 400 pulses per minute constant rate throughout the experiments. The heart was surrounded by a water-jacketed organ bath for maintenance of constant temperature for 30 min. The buffer was pre-filtered to particle size of <0.11 μm and bubbled continuously with 95% O_2 and 5% CO_2 at 37 ℃. Air bubble trap (Physio-Tech Co. Ltd., Tokyo, Japan) and 0.45 μm pore filter (Merck Millipore Ltd., Darmstadt, Germany) were equipped in forward of blunted needle to avoid air embolization. Coronary flow was continuously measured using flowmeter (FLSC-01, Primetech. Corp Ltd., Tokyo, Japan) placed in the aortic perfusion line. The flowmeter was monitored by a computer-based analysis system in Mac-Lab and Chart 7.0 software.[5] All chemicals were applied by infusion method with accurate final concentration.

Hydralazine and metformin treatment

Twelve week-old control$_{\alpha1}^{f/f}{}_{\alpha2}^{f/f}$ and eAMPK$_{\alpha1}^{-/-}{}_{\alpha2}^{-/-}$ mice were treated with hydralazine (0.12 mg/L) or metformin (2 mg/mL) in drinking water for 1 month. Telemetry was implanted at week 3 and blood pressure was measured at week 4.

Immunofluorescence staining

The aorta, mesentery and heart were washed in PBS containing sucrose, and the samples were embedded in OCT compound and quickly frozen. The tissues were cut into 10-μm thick slices. Anti-CD31 (BD Pharmingen) and anti-AMPK (ab80039, Abcam) antibodies were applied at a dilution of 1:1000 and incubated overnight at 4º C, followed by incubation with secondary antibodies 1 hour at room temperature. Slides were viewed in ZEN software with a fluorescence microscopy (LSM 780, Carl Zeiss, Oberkochen, Germany).

Glucose tolerance tests

eAMPK$_{\alpha1}^{-/-}{}_{\alpha2}^{-/-}$ and control $_{\alpha1}^{f/f}{}_{\alpha2}^{f/f}$ mice were fasted overnight for the glucose tolerance test. Glucose (1 g/kg body weight) was injected intraperitoneally and blood was collected from the tail vein at different time points. Blood glucose test was carried out using Glutest-ace (Sanwa Kagaku Kenkyusho Co., Ltd, Nagoya, Japan).

Blood and serum analysis

Blood samples were collected from the right ventricle by direct punctuation and 300-400 μl of the sample were mixed in 3-4 μL of 0.5 mmol/L EDTA. Blood cell counts were determined using a multi-automatic blood cell counter for animals with mouse species program (MICROS LC-152, Horiba, France). The remaining blood samples were put 15 min in room temperature and collected the serum by centrifugation (3000 rpm, 15 min, 4 °C). Serum levels of lipids were analyzed with high-performance liquid chromatography system by Skylight Biotech (Tokyo, Japan).

Histological Analysis

Histological analyses were performed in mice at 16-20 weeks old. The whole mice heart was fixed with 10% buffered formalin for 24-48 hours, then embedded in paraffin wax, and was cut into 3-μm-thick sections that were perpendicular to the long axis of the LV. The sections were then stained with hematoxylin-eosin according to standard histological procedures. For each animal, 20 points were measured for the wall thickness of the LV and the average was calculated. A computer-aided manipulator program (KS-Analyzer v 2.10, Keyence Corp., Osaka, Japan) was used for the analysis.

Chemicals and reagents

N^{ω}-nitro-L-arginine (L-NNA), indomethacin, apamin, (R)-(-)-phenylephrine hydrochloride (PE), acetylcholine (ACh), bradykinin (BK), hydralazine hydrochloride were purchased from Sigma-Aldrich (St. Louis, MO, USA), metformin from LKT laboratories, Inc. (St. Paul, MN, USA), and charybdotoxin from Peptide Institute, Inc. (Osaka, Japan). Indomethacin was dissolved in 10 mmol/L Na_2CO_3. Other drugs dissolved in distillated water were stocked as 1-10 mmol/L solutions. All chemicals and materials of the highest grade available commercially were used at the following final concentrations: PE (1 μmol/L), BK (1 μmol/L), L-NNA (100 μmol/L), a non-

selective NOS inhibitor; indomethacin (10 μmol/L), apamin (100 nmol/L), a small-conductance K_{Ca} channel (SK_{Ca}) blocker; charybdotoxin (100 nmol/L), an intermediate (IK_{Ca})- and a large-(BK_{Ca}) conductance K_{Ca} blocker. PE was used for precontraction of the arteries.

Statistical analysis.

Data analysis was performed by using IBM SPSS Statistics software version 21 (IBM, Armonk, New York, USA). Data are shown as mean ± SEM. Dose-response curves were analyzed by 2-way ANOVA followed by LSD post-hoc test for multiple comparisons. All variables were analyzed by independent paired t-test. $P<0.05$ was considered to be statistically significant.

References

1. Jorgensen SB, Viollet B, Andreelli F, Frosig C, Birk JB, Schjerling P, Vaulont S, Richter EA, Wojtaszewski JF. Knockout of the alpha2 but not alpha1 5'-AMP-activated protein kinase isoform abolishes 5-aminoimidazole-4-carboxamide-1-β-4-ribofuranosidebut not contraction-induced glucose uptake in skeletal muscle. *J Biol Chem*. 2004;279:1070-1079.

2. Kisanuki YY, Hammer RE, Miyazaki J, Williams SC, Richardson JA, Yanagisawa M. Tie2-Cre transgenic mice: A new model for endothelial cell-lineage analysis in vivo. *Dev Biol*. 2001;230:230-242.

3. Enkhjargal B, Hashimoto M, Sakai Y, Shido O. Characterization of vasoconstrictor-induced relaxation in the cerebral basilar artery. *Eur J Pharmacol*. 2010;637:118-123.

4. Nakajima S, Ohashi J, Sawada A, Noda K, Fukumoto Y, Shimokawa H. Essential role of bone marrow for microvascular endothelial and metabolic functions in mice. *Circ Res*. 2012;111:87-96.

5. Ohashi J, Sawada A, Nakajima S, Noda K, Takaki A, Shimokawa H. Mechanisms for enhanced endothelium-derived hyperpolarizing factor-mediated responses in microvessels in mice. *Circ J*. 2012;76:1768-1779.

Supplemental Materials

Legends to Supplemental Figures

Supplemental Figure I. Characterization of eAMPK-KO mice
A. Genotypes of background mice including AMPK floxed (f), Tie2-Cre (Tie2), heterozeguos (h) mice, and control$_{\alpha1}^{f/f}{}_{\alpha2}^{f/f}$ (1), eAMPK$_{\alpha1}^{-/-}{}_{\alpha2}^{-/-}$ (2), control$_{\alpha1}^{f/f}{}_{\alpha2}^{+/+}$ (3), eAMPK$_{\alpha1}^{-/-}{}_{\alpha2}^{+/+}$ (4), control$_{\alpha1}^{+/+}{}_{\alpha2}^{f/f}$ (5), eAMPK$_{\alpha1}^{+/+}{}_{\alpha2}^{-/-}$ (6) mice. **B.** Glucose tolerance test (GTT) in the eAMPK$_{\alpha1}^{-/-}{}_{\alpha2}^{-/-}$ and control$_{\alpha1}^{f/f}{}_{\alpha2}^{f/f}$ mice (n=5 each). Results are expressed as mean±SEM.

Supplemental Figure II. Elevated systolic and diastolic blood pressure in eAMPK-KO mice
Telemetric blood pressure monitoring in (**A**) eAMPK$_{\alpha1}^{-/-}{}_{\alpha2}^{-/-}$ vs. control$_{\alpha1}^{f/f}{}_{\alpha2}^{f/f}$, (**B**) eAMPK$_{\alpha1}^{-/-}{}_{\alpha2}^{+/+}$ vs. control$_{\alpha1}^{f/f}{}_{\alpha2}^{+/+}$ and (**C**) eAMPK$_{\alpha1}^{+/+}{}_{\alpha2}^{-/-}$ vs. control$_{\alpha1}^{+/+}{}_{\alpha2}^{f/f}$ (n=5~6 each). Data are presented as SBP (left) and DBP (right) during 24 hours recording. Results are expressed as mean±SEM. **P*<0.05 vs. control.

Supplemental Figure III. Heart rate in eAMPK-KO mice
Telemetric heart rate monitoring in (**A**) eAMPK$_{\alpha1}^{-/-}{}_{\alpha2}^{-/-}$ vs. control$_{\alpha1}^{f/f}{}_{\alpha2}^{f/f}$, (**B**) eAMPK$_{\alpha1}^{-/-}{}_{\alpha2}^{+/+}$ vs. control$_{\alpha1}^{f/f}{}_{\alpha2}^{+/+}$ and (**C**) eAMPK$_{\alpha1}^{+/+}{}_{\alpha2}^{-/-}$ vs. control$_{\alpha1}^{+/+}{}_{\alpha2}^{f/f}$ (n=5~6 each). Data are presented as heart rate during 24 hours recording (left) and time-averaged heart rate (right). Results are expressed as mean±SEM.

Supplemental Figure IV. Hydralazine and metformin failed to ameliorate LV hypertrophy in eAMPK$_{\alpha1}^{-/-}{}_{\alpha2}^{-/-}$ mice
Telemetric blood pressure monitoring in eAMPK$_{\alpha1}^{-/-}{}_{\alpha2}^{-/-}$, hydralazine and metformin -treated eAMPK$_{\alpha1}^{-/-}{}_{\alpha2}^{-/-}$ and control$_{\alpha1}^{f/f}{}_{\alpha2}^{f/f}$ mice. **A.** Mean arterial pressure (MAP) during 24 hours recording (left) and time-averaged MAP (right). **B.** Systolic (SBP), diastolic (DBP) blood pressure during 24 hours recording (left) and time-averaged SBP and DBP (right). **C.** Heart rate during 24 hours recording (left) and time-averaged heart rate (right). **D.** Histologic analysis of LV hypertrophy. (n=4-5 each). Results are expressed as mean±SEM. **P*<0.05 vs. control$_{\alpha1}^{f/f}{}_{\alpha2}^{f/f}$. †*P*<0.05 vs. eAMPK$_{\alpha1}^{-/-}{}_{\alpha2}^{-/-}$ mice.

Supplemental Figure V. Contracting responses to KCl
Standard contractile responses to 60 mmol/L of KCl (n=10 each). Results are expressed as mean ±SEM.

Supplemental Figure VI. Endothelium-dependent relaxations of the aorta of eAMPK-KO and control mice.

Endothelium-dependent relaxations to acetylcholine (ACh) in (**A**) eAMPK$_{\alpha1}^{-/-}{}_{\alpha2}^{-/-}$ vs. control$_{\alpha1}^{f/f}{}_{\alpha2}^{f/f}$, (**B**) eAMPK$_{\alpha1}^{-/-}{}_{\alpha2}^{+/+}$ vs. control$_{\alpha1}^{f/f}{}_{\alpha2}^{+/+}$ and (**C**) eAMPK$_{\alpha1}^{+/+}{}_{\alpha2}^{-/-}$ vs. control$_{\alpha1}^{+/+}{}_{\alpha2}^{f/f}$ mice (n=7~10 each) in the absence (circle) and the presence of indomethacin (square, Indo), indomethacin plus N$^{\omega}$-nitro-L-arginine (triangle, L-NNA), and indomethacin, L-NNA plus charybdotoxin (CTx) and apamin (lozenge, Apm). Data are presented as dose-dependent responses (left) and area under the curve (right). Results are expressed as mean±SEM.

Supplemental Figure VII. Endothelium-dependent relaxations in hydralazine-treated mice

Endothelium-dependent responses to acetylcholine (ACh) of the aorta (**A**) and mesenteric arteries (**B**) after hydralazine treatment in eAMPK$_{\alpha1}^{-/-}{}_{\alpha2}^{-/-}$ (n=7 each) vs. control$_{\alpha1}^{f/f}{}_{\alpha2}^{f/f}$ mice (n=4) in the absence (circle) and the presence of indomethacin (square, Indo), indomethacin plus N$^{\omega}$-nitro-L-arginine (triangle, L-NNA), and indomethacin, L-NNA plus charybdotoxin (CTx) and apamin (lozenge, Apm). Data are presented as dose-dependent responses (left) and area under the curve (right). Results are expressed as mean±SEM. ***P*<0.01.

Supplemental Figure VIII. Endothelium-dependent relaxations in metformin-treated mice

Endothelium-dependent responses to acetylcholine of the aorta (**Ao**) and mesenteric arteries (**B**) after metformin treatment in eAMPK$_{\alpha1}^{-/-}{}_{\alpha2}^{-/-}$ and control$_{\alpha1}^{f/f}{}_{\alpha2}^{f/f}$ mice (n=6 each) in the absence (circle) and the presence of indomethacin (square, Indo), indomethacin plus N$^{\omega}$-nitro-L-arginine (triangle, L-NNA), and indomethacin, L-NNA plus charybdotoxin (CTx) and apamin (lozenge, Apm). Data are presented as dose-dependent responses (left) and area under the curve (right). Results are expressed as mean±SEM. ***P*<0.01.

Supplemental Figure IX. Endothelium-independent relaxations to sodium nitroprusside

Endothelium-independent relaxations to sodium nitroprusside (SNP) in (**A**) eAMPK$_{\alpha1}^{-/-}{}_{\alpha2}^{-/-}$ vs. control$_{\alpha1}^{f/f}{}_{\alpha2}^{f/f}$, (**B**) eAMPK$_{\alpha1}^{-/-}{}_{\alpha2}^{+/+}$ vs. control$_{\alpha1}^{f/f}{}_{\alpha2}^{+/+}$ and (**C**) eAMPK$_{\alpha1}^{+/+}{}_{\alpha2}^{-/-}$ vs. control$_{\alpha1}^{+/+}{}_{\alpha2}^{f/f}$ mice (n=10 each). Results are expressed as mean±SEM. **P*<0.05 vs. control.

Supplemental Figure X. Endothelium-independent relaxations to NS-1619

Endothelium-independent relaxations to NS-1619 in (**A**) eAMPK$_{\alpha1}^{-/-}{}_{\alpha2}^{-/-}$ vs. control$_{\alpha1}^{f/f}{}_{\alpha2}^{f/f}$, (**B**) eAMPK$_{\alpha1}^{-/-}{}_{\alpha2}^{+/+}$ vs. control$_{\alpha1}^{f/f}{}_{\alpha2}^{+/+}$ and (**C**) eAMPK$_{\alpha1}^{+/+}{}_{\alpha2}^{-/-}$ vs. control$_{\alpha1}^{+/+}{}_{\alpha2}^{f/f}$ mice (n=4-5 each). Results are expressed as mean±SEM.

Supplemental Figure XI. Endothelium-independent relaxations to exogenous H_2O_2
Endothelium-independent relaxations to exogenous H_2O_2 in (**A**) $eAMPK_{\alpha1}^{-/-}{}_{\alpha2}^{-/-}$ vs. $control_{\alpha1}^{f/f}{}_{\alpha2}^{f/f}$, (**B**) $eAMPK_{\alpha1}^{-/-}{}_{\alpha2}^{+/+}$ vs. $control_{\alpha1}^{f/f}{}_{\alpha2}^{+/+}$ and (**C**) $eAMPK_{\alpha1}^{+/+}{}_{\alpha2}^{-/-}$ vs. $control_{\alpha1}^{+/+}{}_{\alpha2}^{f/f}$ mice (n=4-5 each). Results are expressed as mean ± SEM.

Supplemental Figure XII. Effects of hydralazine treatment on endothelium-independent relaxations
No effects of hydralazine treatment were noted on endothelium-independent relaxations to sodium nitroprusside (SNP) (**A**), NS-1619 (**B**), and exogenous H_2O_2 (**C**) in control and $eAMPK_{\alpha1}^{-/-}{}_{\alpha2}^{-/-}$ mice (n=7 each). Results are expressed as mean ± SEM.

Supplemental Figure XIII. Effects of hydralazine treatment on endothelium-independent relaxations
No effects of hydralazine treatment were noted on endothelium-independent relaxations to sodium nitroprusside (SNP) (**A**), NS-1619 (**B**), and exogenous H_2O_2 (**C**) in control (n=6) and $eAMPK_{\alpha1}^{-/-}{}_{\alpha2}^{-/-}$ mice (n=7). Results are expressed as mean ± SEM.

Supplemental Figure I

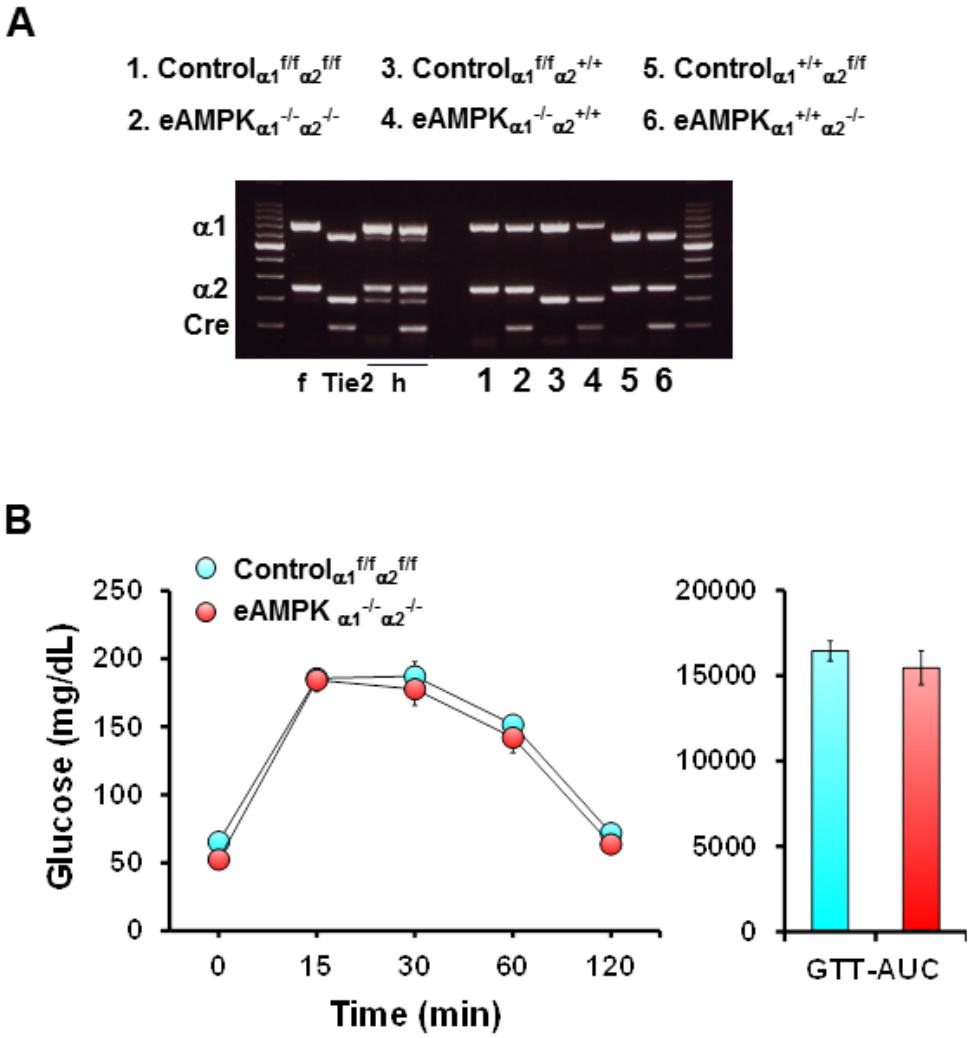

Supplemental Figure II

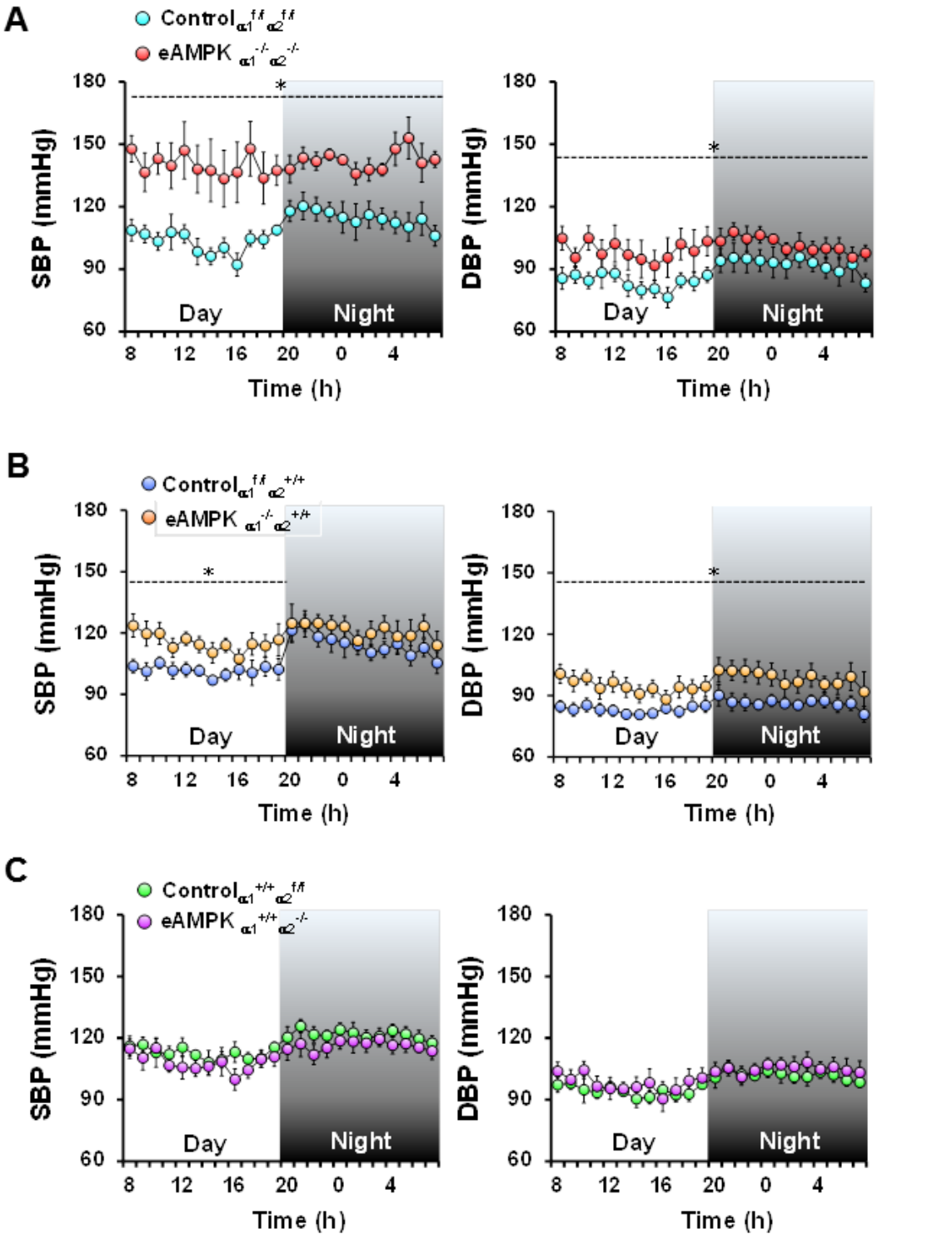

Supplemental Figure III

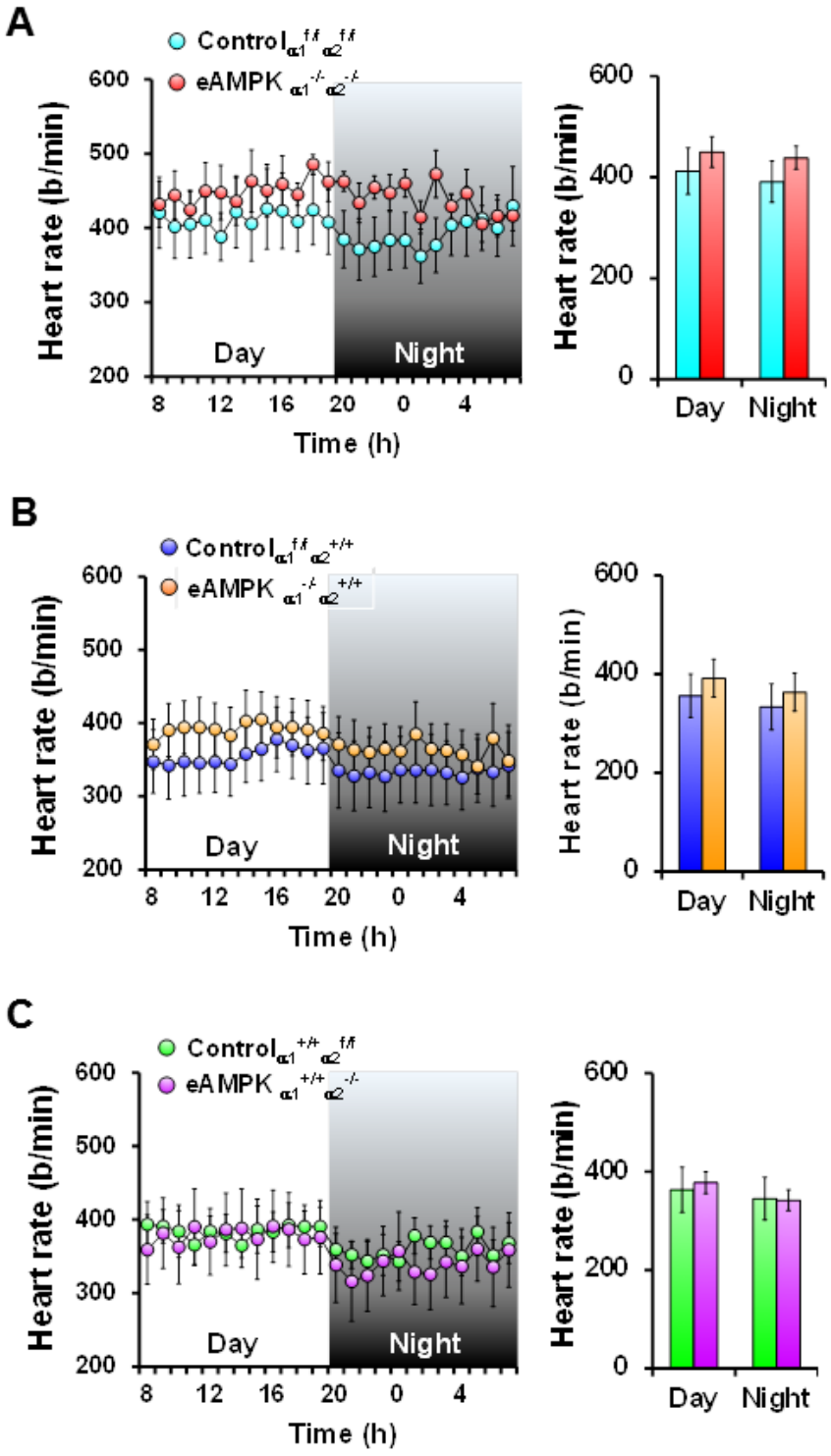

Supplemental Figure IV

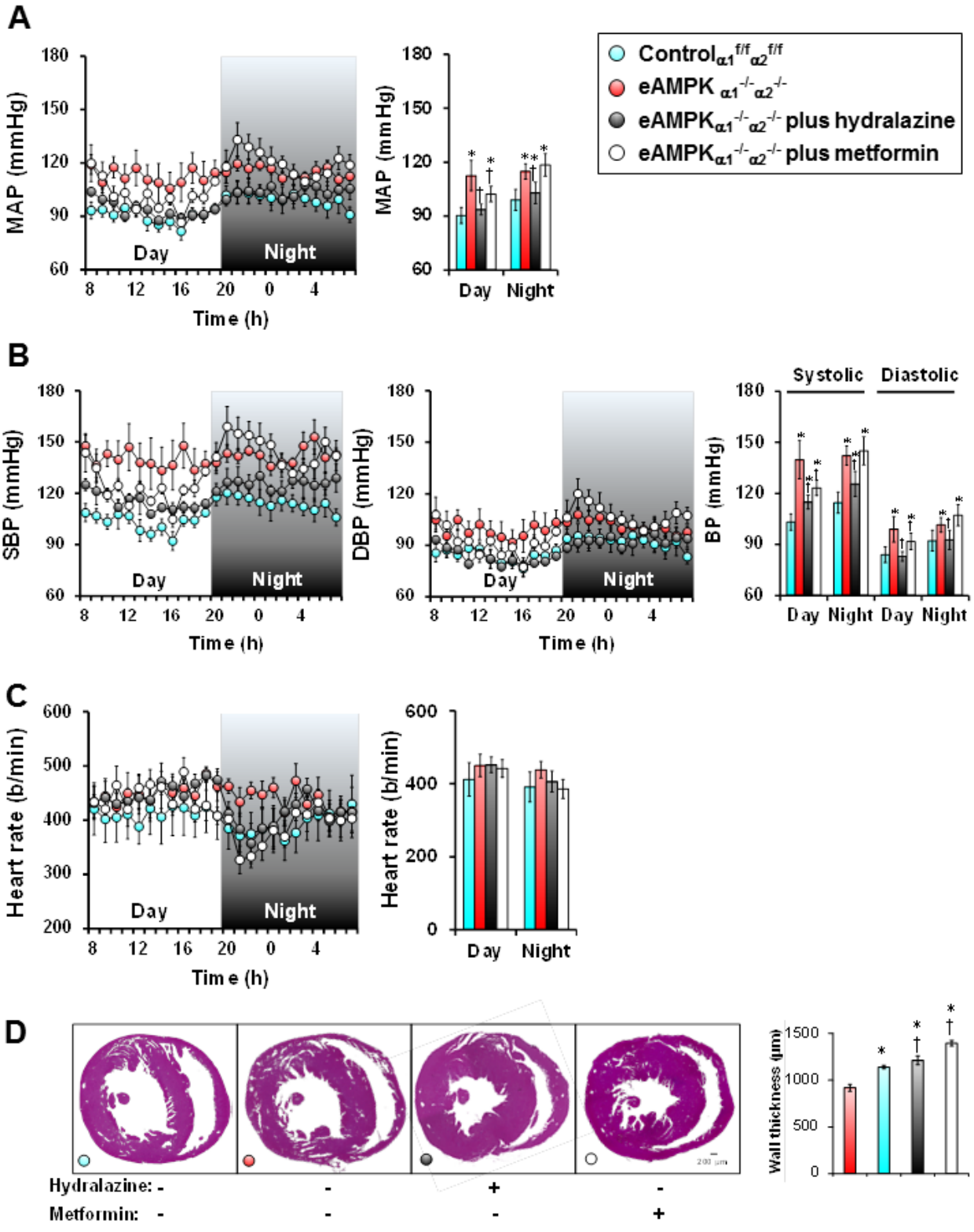

Supplemental Figure V

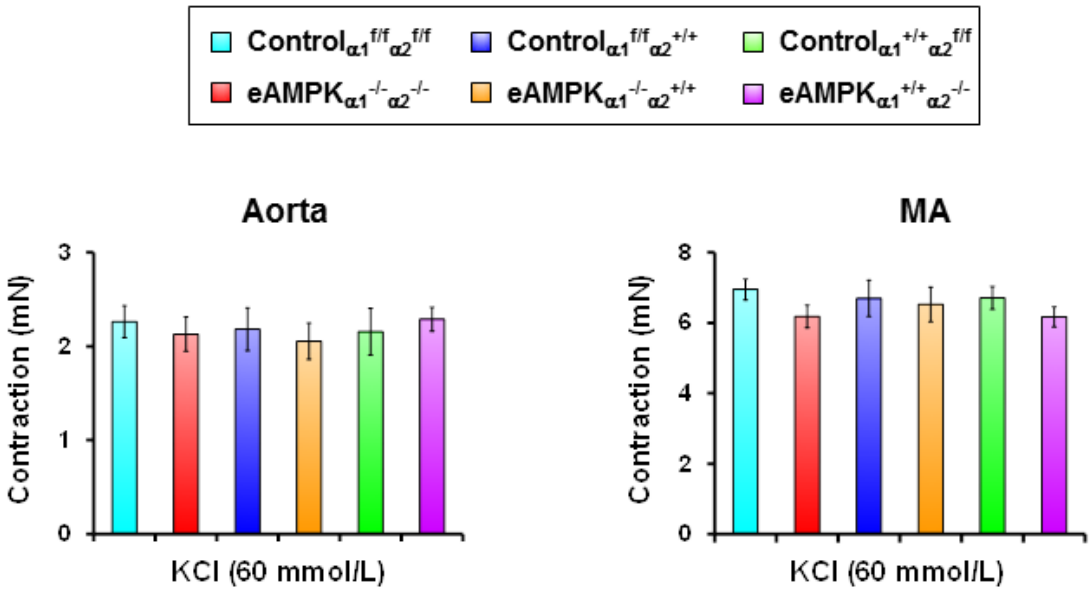

Supplemental Figure VI

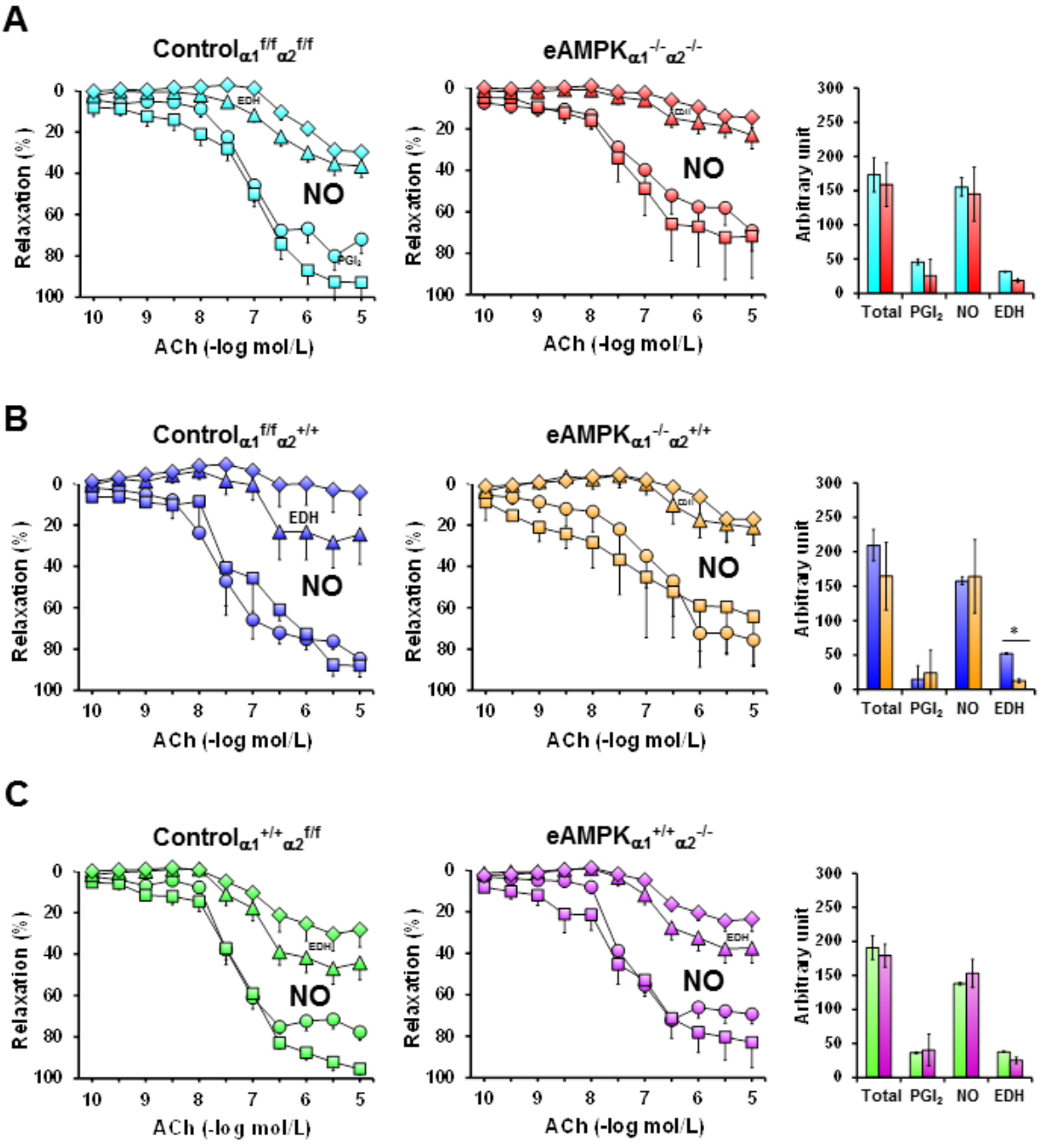

Supplemental Figure VII

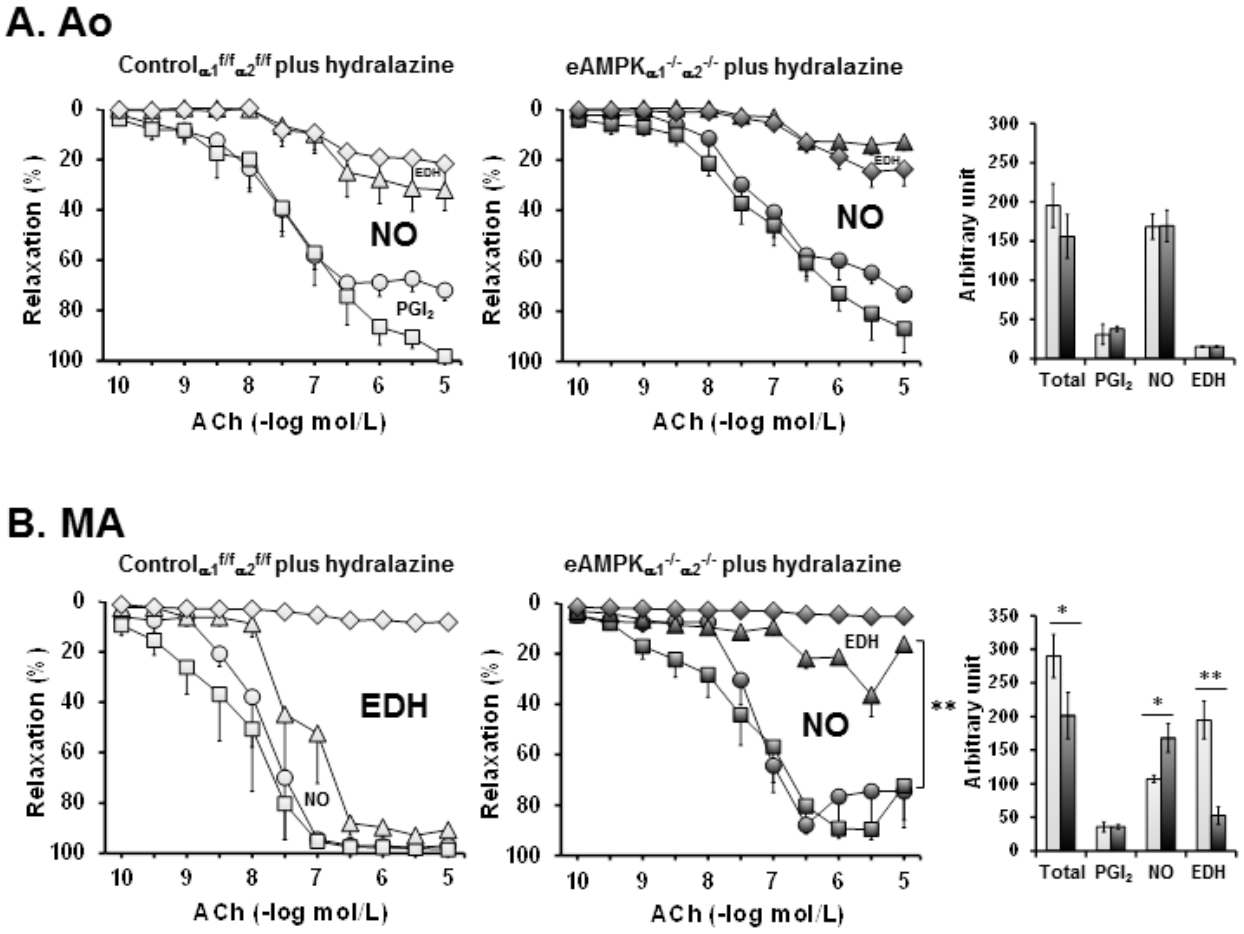

Supplemental Figure VIII

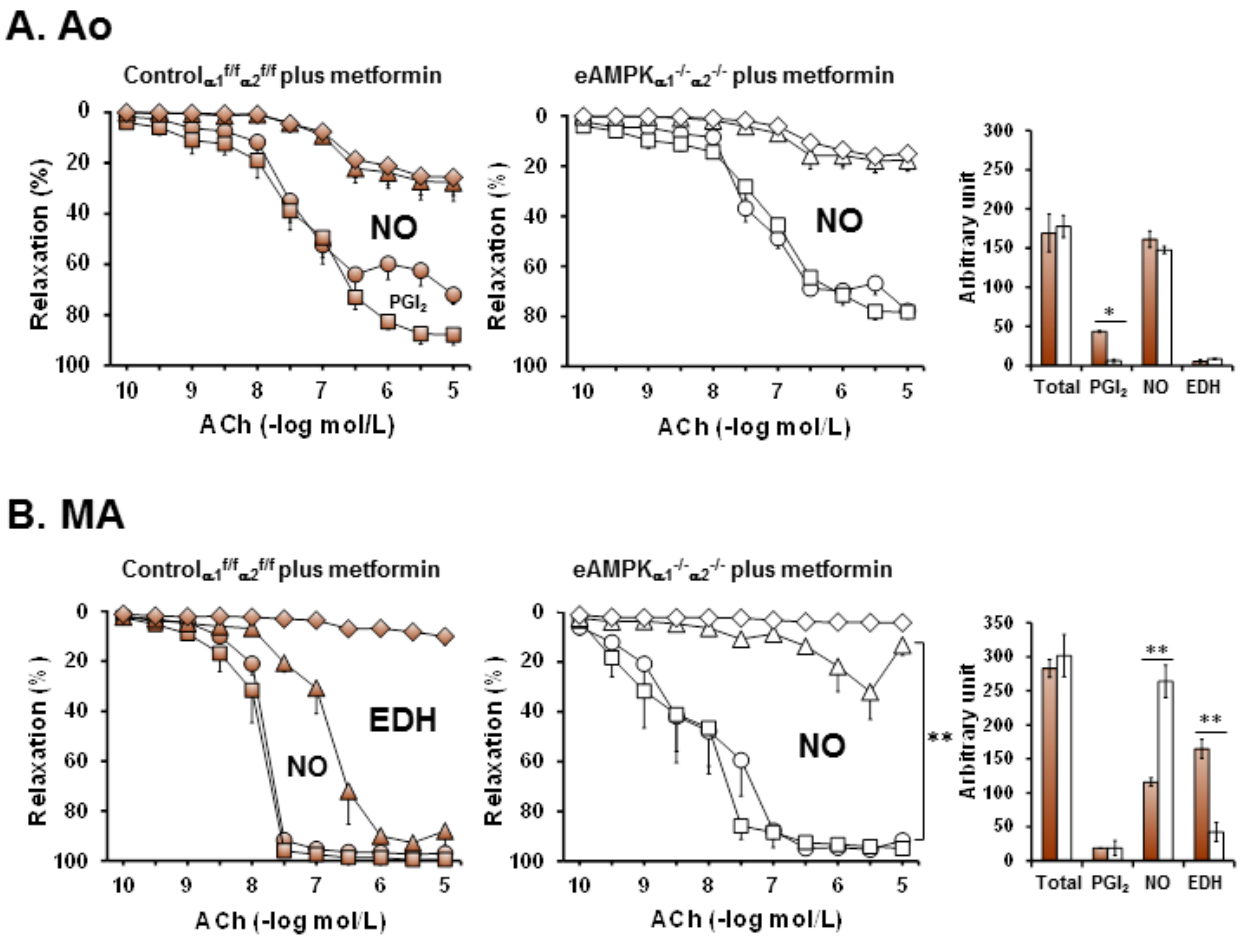

Supplemental Figure IX

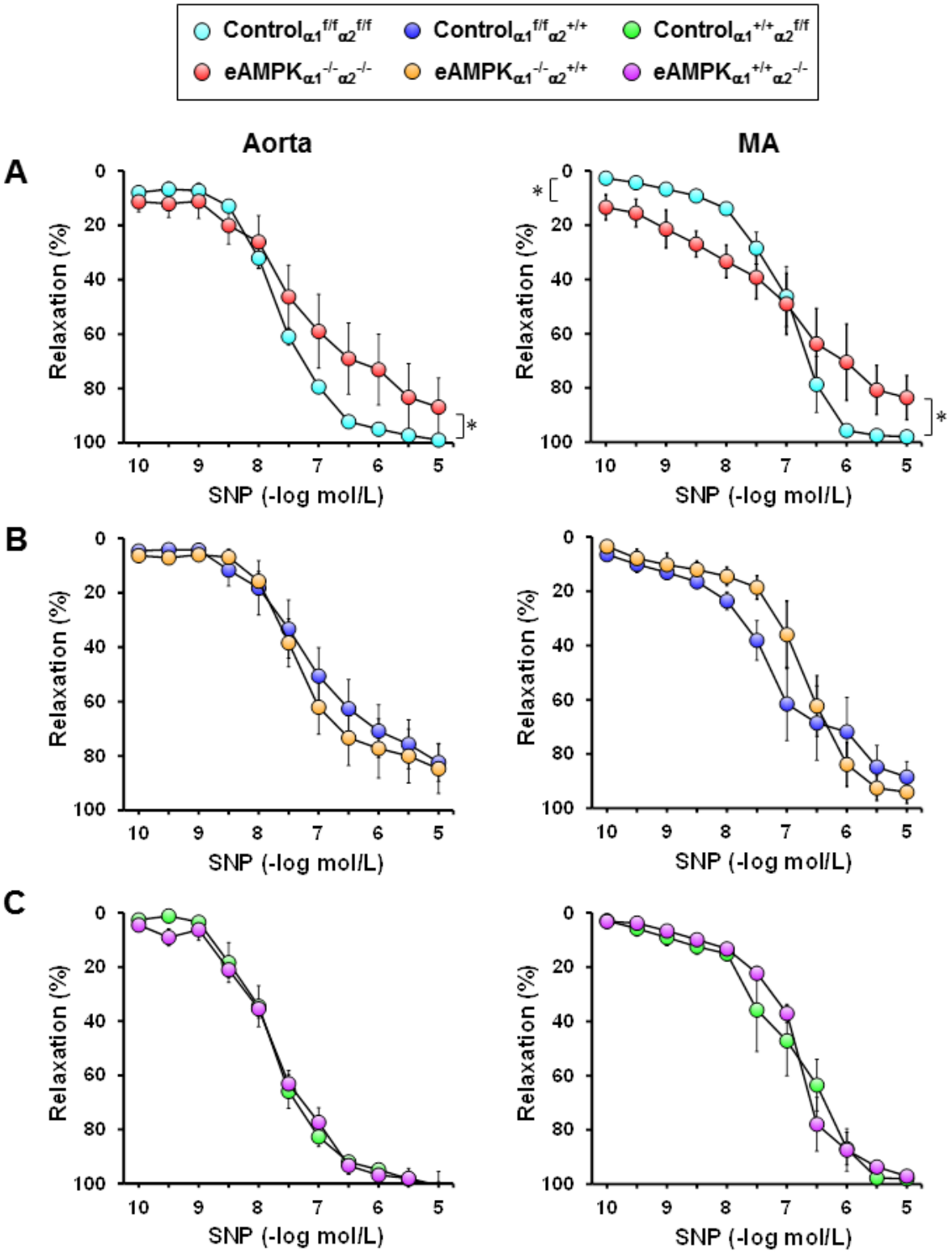

Supplemental Figure X

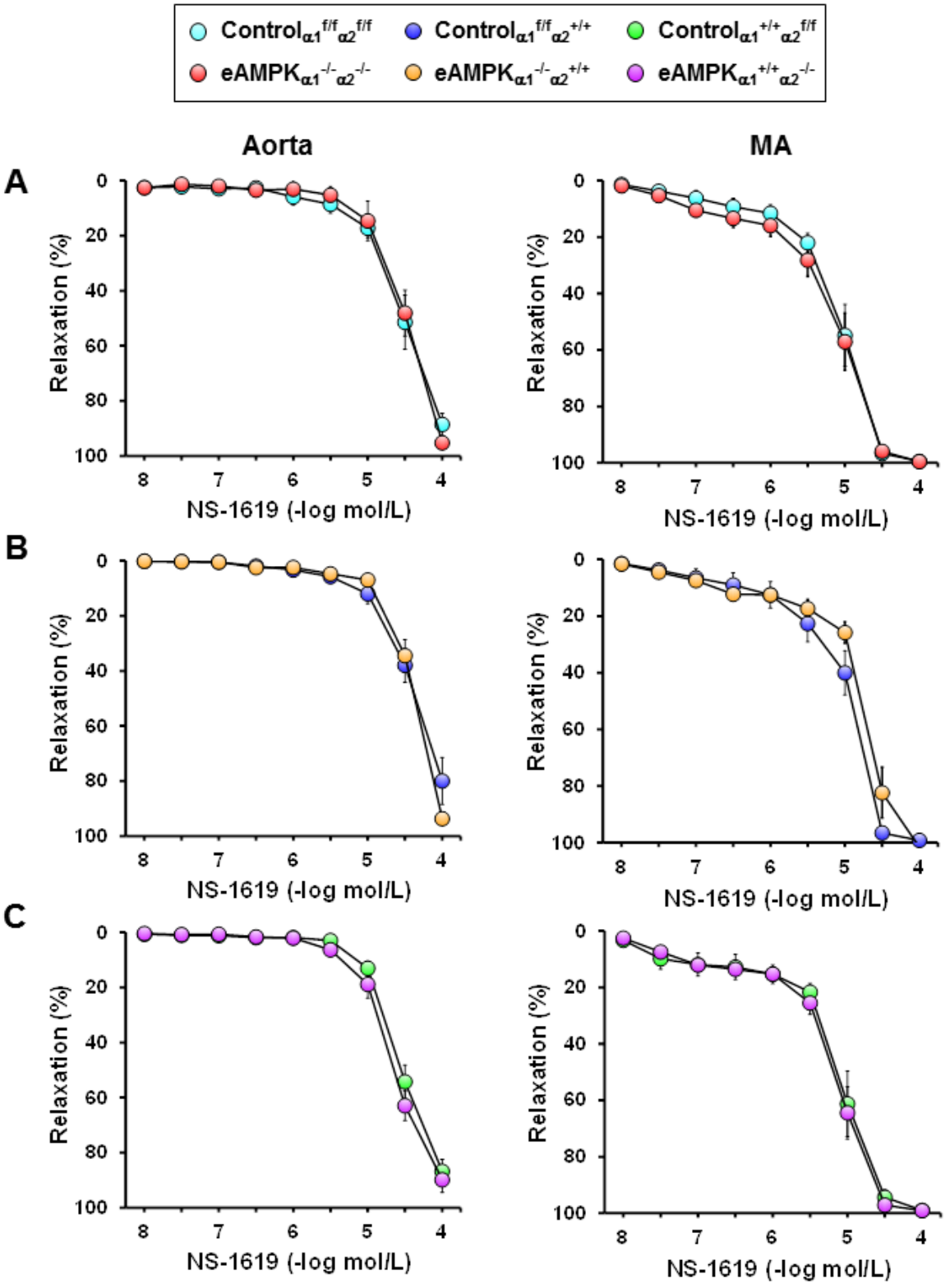

Supplemental Figure XI

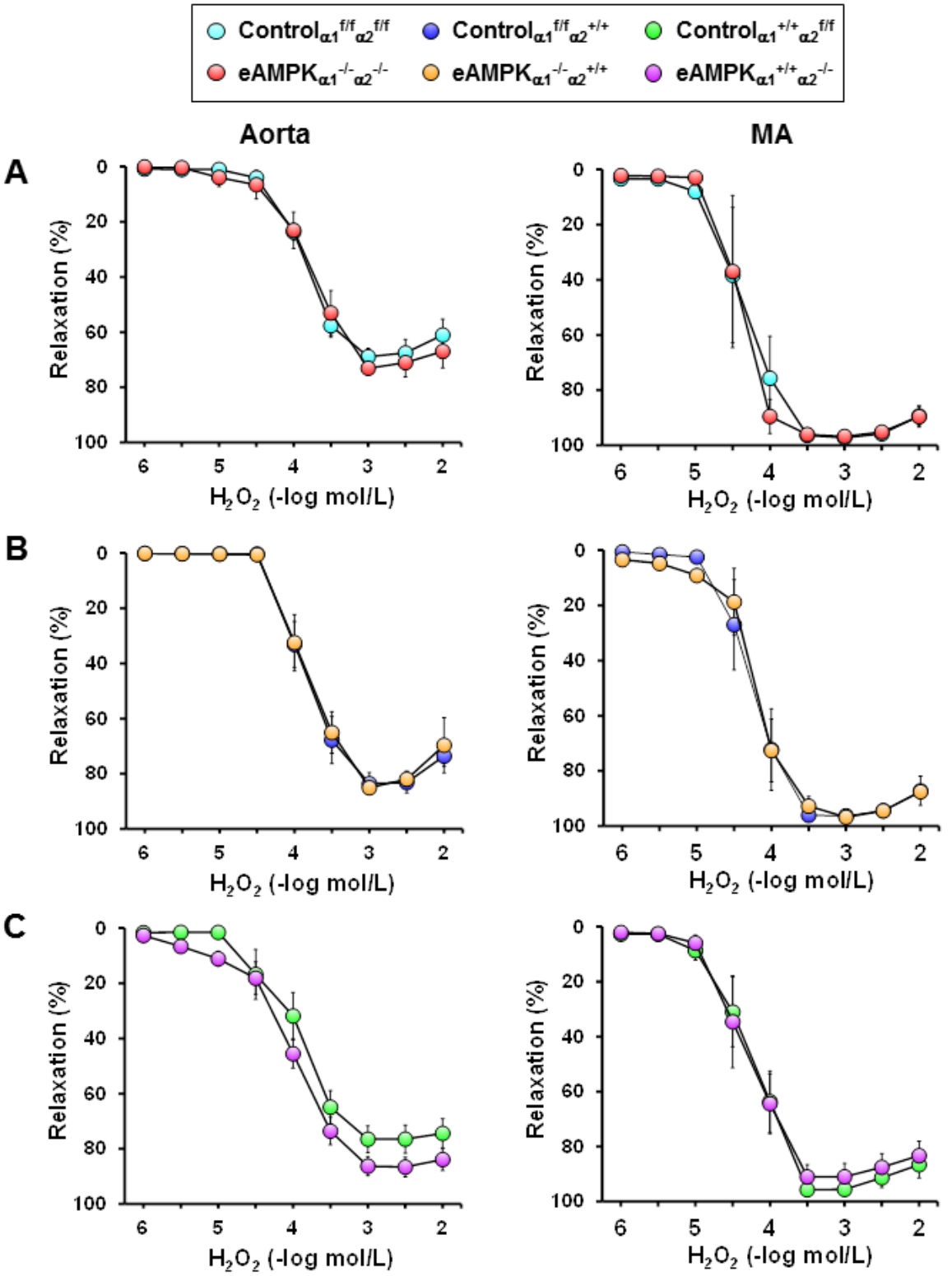

Supplemental Figure XII

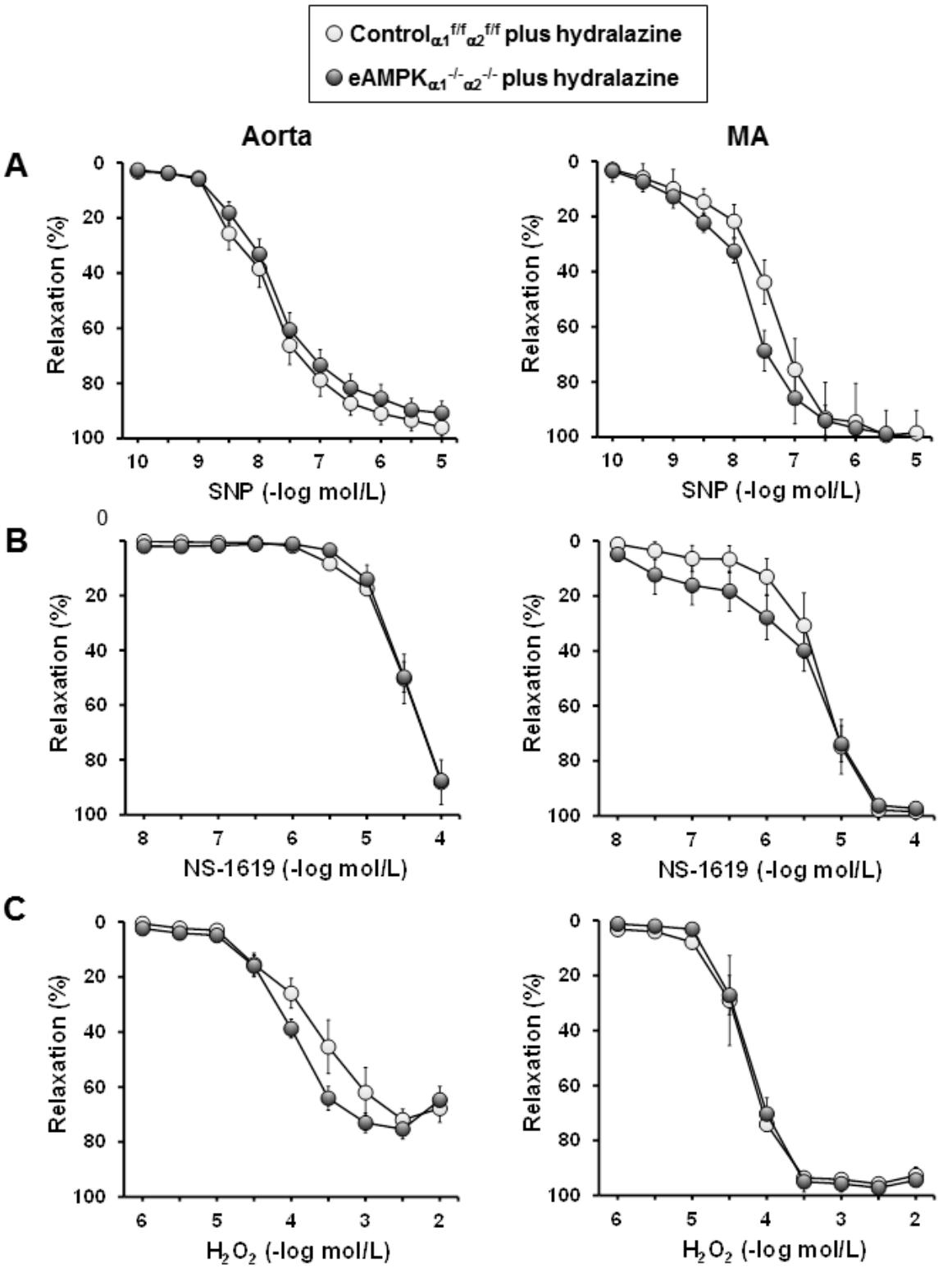

Supplemental Figure XIII

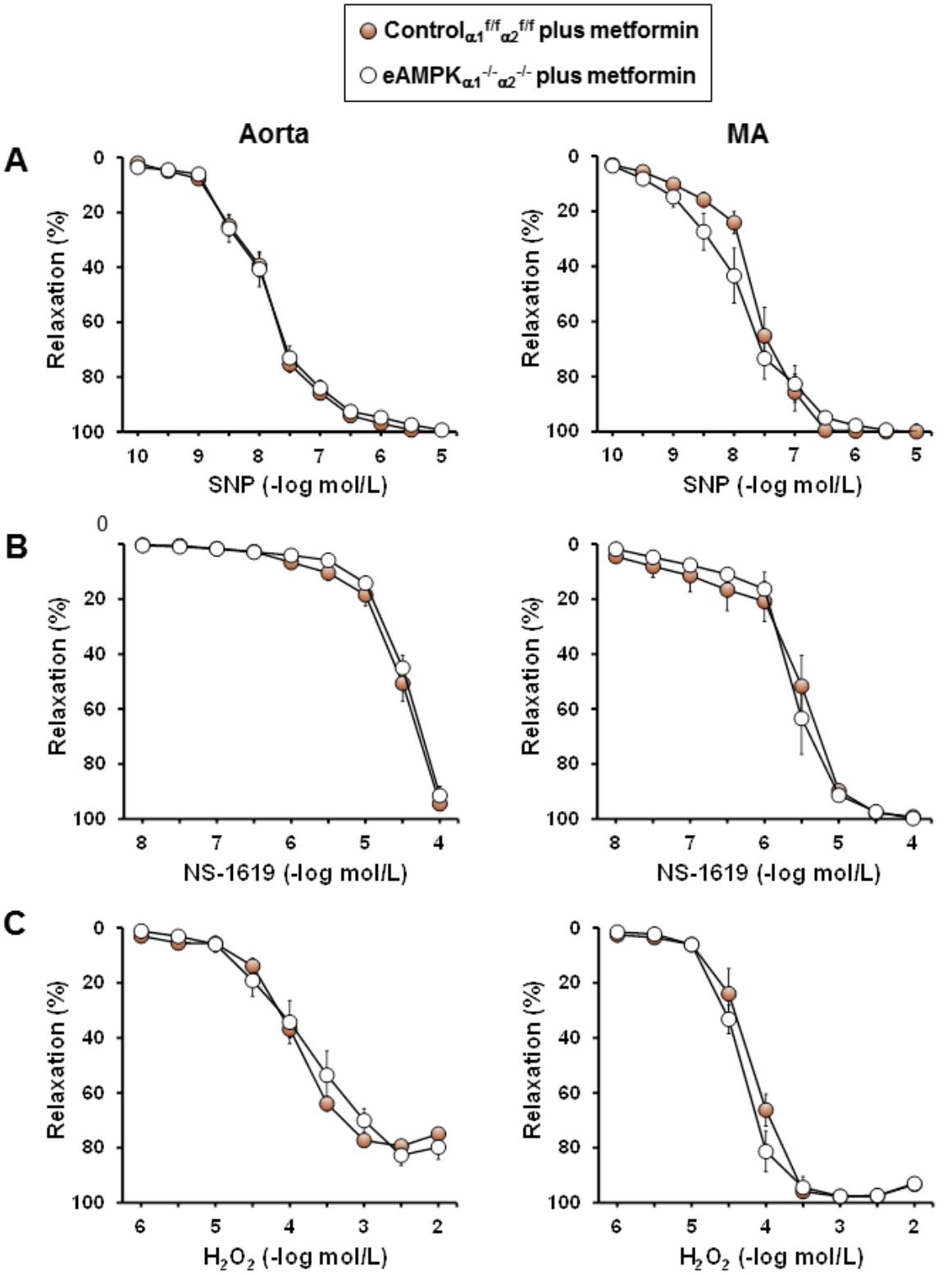

Supplemental Table I. Characteristics of eAMPK-KO and control mice

Groups	Control$_{\alpha1}^{f/f}{}_{\alpha2}^{f/f}$	eAMPK$_{\alpha1}^{-/-}{}_{\alpha2}^{-/-}$	Control$_{\alpha1}^{f/f}{}_{\alpha2}^{+/+}$	eAMPK$_{\alpha1}^{-/-}{}_{\alpha2}^{+/+}$	Control$_{\alpha1}^{+/+}{}_{\alpha2}^{f/f}$	eAMPK$_{\alpha1}^{+/+}{}_{\alpha2}^{-/-}$
Body weight (g)						
12 weeks	29.7 ± 0.8	28.2 ± 0.7	32.7 ± 0.5	31.2 ± 0.7	27.6 ± 0.7	28.0 ± 0.9
13 weeks	30.1 ± 0.7	29.6 ± 0.6	33.4 ± 0.7	30.7 ± 0.8*	28.8 ± 0.6	28.9 ± 0.9
14 weeks	32.8 ± 0.8	29.9 ± 0.5*	34.1 ± 0.7	31.5 ± 0.9**	29.0 ± 0.5	30.1 ± 0.6
15 weeks	32.8 ± 0.8	30.6 ± 0.7*	34.9 ± 0.6	32.4 ± 0.5**	29.1 ± 0.6	29.0 ± 0.7
16 weeks	33.3 ± 1.2	30.1 ± 0.7*	34.2 ± 0.4	31.3 ± 1.3**	29.6 ± 0.6	30.2 ± 0.7
17 weeks	34.9 ± 0.9	29.6 ± 1.4**	35.3 ± 0.8	31.5 ± 1.2**	30.7 ± 0.7	30.3 ± 1.0
Organs/BW (mg/g)						
Heart/BW	4.9 ± 0.1	5.4 ± 0.2*	4.7 ± 0.2	5.4 ± 0.3**	4.9 ± 0.1	5.0 ± 0.1
Lung/BW	5.1 ± 0.2	5.4 ± 0.2	4.8 ± 0.2	4.8 ± 0.2	4.9 ± 0.2	5.0 ± 0.1
Liver/BW	46.9 ± 1.6	47.6 ± 2.1	47.4 ± 2.4	46.3 ± 1.4	45.2 ± 1.9	45.3 ± 1.9
Kidney/BW	15.1 ± 0.3	14.6 ± 0.4	14.3 ± 0.4	13.5 ± 0.4	14.4 ± 0.4	14.9 ± 0.3
Visceral fat/BW (mg/g)						
Perinephric	7.4 ± 1.2	7.4 ± 1.6	7.4 ± 1.4	6.7 ± 1.5	3.6 ± 0.5	3.4 ± 0.9
Mesenteric	11.2 ± 1.6	13.8 ± 2.4	9.2 ± 1.1	8.9 ± 1.4	6.4 ± 0.8	4.5 ± 1.5
Epididymal	22.3 ± 3.3	21.5 ± 4.0	21.0 ± 2.8	21.0 ± 3.5	13.6 ± 0.9	13.6 ± 2.4
Omentum	8.5 ± 0.5	8.8 ± 0.6	9.4 ± 0.7	9.5 ± 0.5	10.5 ± 0.8	8.8 ± 0.4
Total	50.7 ± 5.4	56.0 ± 7.5	46.9 ± 5.1	48.1 ± 7.1	34.1 ± 1.8	24.2 ± 3.7
Hematology						
WBC (x10^3/mm^3)	2.7 ± 0.4	2.3 ± 0.3	2.5 ± 0.2	3.4 ± 0.5	2.9 ± 0.5	2.5 ± 0.5
RBC (x10^6/mm^3)	9.6 ± 0.2	9.5 ± 0.2	9.6 ± 0.2	9.6 ± 0.3	9.6 ± 0.1	9.4 ± 0.1
HGB (g/dL)	13.5 ± 0.2	13.5 ± 0.2	13.5 ± 0.3	13.1 ± 0.6	13.7 ± 0.2	13.5 ± 0.1
HCT (%)	44.8 ± 0.8	44.7 ± 1.0	44.9 ± 0.8	44.1 ± 2.0	44.8 ± 0.7	43.6 ± 0.4
MCV (x10^{-15}L)	46.6 ± 0.2	47.0 ± 0.2	46.7 ± 0.2	46.1 ± 0.7	46.4 ± 0.3	46.2 ± 0.3
MCH (pg)	14.1 ± 0.1	14.2 ± 0.1	14.1 ± 0.1	13.0 ± 0.2	14.2 ± 0.1	14.3 ± 0.1
MCHC (g/dL)	30.2 ± 0.2	30.0 ± 0.6	30.1 ± 0.1	30.0 ± 0.1	30.7 ± 0.3	31.0 ± 0.2
PLT (x10^3/mm^3)	721.8 ± 48.5	756.6 ± 22.9	744.1 ± 28.9	849.5 ± 62.2	738.9 ± 87.8	662.8 ± 124.7
Lipid levels (mg/dL)						
Total	62.8 ± 4.3	55.7 ± 2.9	82.7 ± 6.1	92.8 ± 4.6	67.5 ± 8.3	64.4 ± 5.6
CM	0.20 ± 0.06	0.24 ± 0.05	0.56 ± 0.23	0.46 ± 0.06	0.30 ± 0.08	0.25 ± 0.11
VLDL	4.2 ± 0.7	4.0 ± 1.0	6.6 ± 1.2	6.7 ± 0.8	3.9 ± 1.9	3.4 ± 1.6
LDL	6.4 ± 1.0	5.1 ± 0.8	11.6 ± 1.8	10.0 ± 1.1	4.8 ± 1.1	4.7 ± 1.0
HDL	52.0 ± 3.1	46.3 ± 2.7	63.9 ± 5.6	75.6 ± 4.5	58.5 ± 8.6	56.2 ± 5.2
TG	51.2 ± 8.8	42.8 ± 9.2	76.3 ± 18.9	79.9 ± 8.1	40.0 ± 14.4	38.0 ± 25.3

Results are expressed as mean±SEM. BW, body weight; WBC, white blood cell; RBC, red blood cel; HGB, hemoglobin; HCT, hematocrit; MCV, mean corpuscular volume; MCH, mean corpuscular hemoglobin; MCHC, mean corpuscular hemoglobin concentration; PLT, platelet; CM, chylomicrons; VLDL, very-low-density lipoprotein; LDL, low-density lipoprotein; HDL, high-density lipoprotein; TG, triglycerides. Control$_{\alpha1}^{f/f}{}_{\alpha2}^{f/f}$, control$_{\alpha1}^{f/f}{}_{\alpha2}^{+/+}$, and control$_{\alpha1}^{+/+}{}_{\alpha2}^{f/f}$, littermate AMPK$_{\alpha1\alpha2}$ subunits-, AMPK$_{\alpha1}$ subunit-, and AMPK$_{\alpha2}$ subunit-floxed mice, respectively. eAMPK$_{\alpha1}^{-/-}{}_{\alpha2}^{-/-}$, , eAMPK$_{\alpha1}^{-/-}{}_{\alpha2}^{+/+}$-, and eAMPK$_{\alpha1}^{+/+}{}_{\alpha2}^{-/-}$, endothelial AMPK$_{\alpha1\alpha2}$ subunits-, AMPK$_{\alpha1}$ subunit-, and AMPK$_{\alpha2}$ subunits-knockout mice, respectively. n= 7-10 in each group. *P<0.05, **P<0.01, ***P<0.001 vs. control.

Supplemental Table II. Effects of hydralazine and metformin treatments on the male eAMPK$_{\alpha1}^{-/-}{}_{\alpha2}^{-/-}$ and control mice.

Groups	Control$_{\alpha1}^{f/f}{}_{\alpha2}^{f/f}$ +hydralazine	eAMPK$_{\alpha1}^{-/-}{}_{\alpha2}^{-/-}$ +hydralazine	Control$_{\alpha1}^{f/f}{}_{\alpha2}^{f/f}$ +metformin	eAMPK$_{\alpha1}^{-/-}{}_{\alpha2}^{-/-}$ +metformin
Body weight (g)				
16 weeks	33.9 ± 1.3	32.6 ± 0.4	33.0 ± 0.6	29.7 ± 1.1*
17 weeks	34.1 ± 0.9	33.7 ± 0.6	33.3 ± 0.8	30.6 ± 1.1
18 weeks	34.1 ± 0.6	34.2 ± 0.7	32.9 ± 0.8	30.3 ± 1.0
Organs/BW (mg/g)				
Heart/BW	5.6 ± 0.4	6.0 ± 0.1*	5.1 ± 0.1	6.0 ± 0.2*
Lung/BW	5.7 ± 0.2	6.7 ± 0.6*	5.4 ± 0.1	5.0 ± 0.1
Liver/BW	58.5 ± 5.7	56.1 ± 1.6	57.3 ± 2.0	56.5 ± 1.4
Kidney/BW	13.2 ± 0.8	13.7 ± 0.3	13.3 ± 0.3	13.5 ± 0.5
Visceral fat/BW (mg/g)				
Perinephric	2.4 ± 0.6	2.0 ± 0.3	3.3 ± 1.5	2.9 ± 0.9
Mesenteric	8.1 ± 1.5	6.5 ± 0.9	8.3 ± 1.4	9.3 ± 2.0
Epididymal	13.3 ± 2.5	11.4 ± 1.6	13.3 ± 3.3	11.7 ± 1.4
Omentum	13.1 ± 1.2	11.6 ± 0.4	11.7 ± 0.5	11.2 ± 1.1
Total	36.8 ± 4.2	31.4 ± 2.5	36.9 ± 6.1	35.1 ± 3.9

Results are expressed as mean±SEM. BW, body weight; control$_{\alpha1}^{f/f}{}_{\alpha2}^{f/f}$, littermate AMPK$\alpha_1\alpha_2$ subunits floxed mice (n=4, plus hydralazine; n=5, plus metformin); eAMPK$_{\alpha1}^{-/-}{}_{\alpha2}^{-/-}$, endothelial AMPK$\alpha_1\alpha_2$ subunits knockout mice (n= 6). *P<0.05 vs. control plus treatment.